Journal of African Earth Sciences 207 (2023) 105048

Contents lists available at ScienceDirect

Journal of African Earth Sciences

journal homepage: www.elsevier.com/locate/jafrearsci

Morphometric and biomorphic variability of theropod footprint characters from Imilchil tracksites (Mid-? Late Jurassic, Central High Atlas, Morocco).

Moussa Masrour [a], Mohamed Boutakiout [b], Judit Minguez Ceniceros [c], Tanguy Rolland [d], Félix Pérez-Lorente [c,e,*]

[a] Université Ibn Zohr, Faculté des Sciences, Dpt. de Géologie, BP8106, Cité Dakhla, Agadir, Morocco
[b] Université Mohamed V, BP1014, RP, Rabat, Morocco
[c] Universidad de La Rioja, Edificio CCT, Madre de Dios 51-53, E-26006, Logroño, Spain
[d] Université de Bourgogne-Franche-Comté, UMR6298 ARTEHIS,Bureau 415 France
[e] Amigos Del Museo de Enciso (AME). Portillo, 3. E-26586 Enciso, Spain

ARTICLE INFO

Handling Editor: DR Damien Delvaux

Keywords:
Dinosaur footprints
Preservation
Numerical data
Bathonian-? callovian

ABSTRACT

This paper presents the study of 14 new sites with theropod footprints in Imilchil. The study focuses on ichnotaxonomic and extramorphological characteristics of the footprints, the analysis of their trackways, and the correlation with the descriptions of published tridactil footprints. The objective has been to provide a comparative view of theropod ichnites with the relationship between the substrate and the footprint (in the interval between its formation and its current state) and the ichnotaxonomic data. The distribution of footprints in true or real footprints (including stamps and deformed footprints), undertracks, subtracks, and eroded footprints is introduced, and the variation in their morphological characters due to preservation processes is analyzed. An exposition of the analysis of the measurements of footprints and trackways has also been made, comparing them with data obtained in two other large sites studied and known by the team (La Rioja and Iouaridène). The numerical data confirm the generality of some of the previous and little-known observations of the repetition of distributions related to the metric of dinosaur footprints and trackways.

1. Introduction

The Imilchil ensemble of paleoichnological sites contains ichnites of tetrapods (including dinosaurs, crocodiles, pterosaurs) from the Middle-? Late Jurassic age (Charrière et al., 2011) whose features have been highlighted in several publications (cf. Minguez Ceniceros et al., 2022). The prospecting and study of the new outcrops have provided data that serve for the critical analysis of all the Imilchil sites and their content. In this study, we take into consideration the importance of the interpretation of the footprint morphology (Sarjeant, 1989, 1990) in the process of the footprint formation. This method of study is more comprehensive than that based on the analysis of footprints exclusively as zoologically classifiable elements.

We studied the theropod footprints (*sensu* Thulborn, 1990; Romero-Molina et al., 2003 [see Minguez Ceniceros et al., 2022]) and their trackways and distributions from a total of 14 sites in locations other than those studied by teams that have worked in the area. The biomorphic and morphometric footprint data have been compared with the ichnotaxa described in Imilchil, and the data associated with their trackways have been compared with those published by various authors.

The footprints and trackways are examined taking into account:

i) the ichnotaxonomic classification of dinosaur footprints known in the area (cf. Klein et al., 2022);
ii) the irregularities and deformations produced during the phases (T, touch-down phase; W,weight-bearing phase; K, kick-off phase) of the footprint formation (Thulborn and Wade, 1989) and in the subsequent transformations (synsedimentary movements, weathering and erosion) and;
iii) the relationship of the metric data variation (Pérez-Lorente, 1996) from other countries.

The footprint deformation produced by post-sedimentary compaction and diagenesis is not appreciable from the morphology of the

* Corresponding author. Universidad de La Rioja, Edificio CCT, Madre de Dios 51-53, E-26006, Logroño, Spain.
E-mail addresses: moussamasrour5@gmail.com (M. Masrour), mboutakiout@gmail.com (M. Boutakiout), judit.minguez@unirioja.es (J. Minguez Ceniceros), tanguy.rolland@u-bourgogne.fr (T. Rolland), felix.perez@unirioja.es (F. Pérez-Lorente).

https://doi.org/10.1016/j.jafrearsci.2023.105048
Received 22 March 2023; Received in revised form 11 August 2023; Accepted 28 August 2023
Available online 2 September 2023
1464-343X/

Table 1
Imilchil TAG sites, coordinates, strike and slip of the study surface, number of footprints, trackways, pairs and isolated footprints.

Site	UTM	Strike/dip// area (m^2)	number of: footprints// trackways//pairs//isolate footprints
7.10TAG	262575// 3562686	N90/25S/56	35t, 8s, 9ct//6t//1t//2t,8s
7.8TAG	262583// 3562674	N102/27S// 18	28t//1//4//17
7.7TAG	262582// 3562674	N90/24S//39	67t//12//2//5
7.6TAG	262919// 3562695	N83/25S//52	9t//1//0//6
7.5TAG	263241// 3562871	N80/33S//22	7t, 18s//1t, 2s//0//2t
74TAG	263213// 3562742	N80/30S//28	27t, 12s//5t, 1s//3t//5t,2s
7.3TAG	263250// 3562684	N75/28S//36	41t//3//5//19
7.2TAG	262026// 3561585	N92/36S//63	8t, 13s//2t,1s//1t//0
7.1TAG	260750// 3562147	N105/38S// 24	18t//3//0//0
5.1TAG	260998// 3561396	N80/30S//1	58t//6//4//12
4.5TAG	261328// 3562481		1t//0//0//1
4.3TAG	261271// 3562499	N80/34S//13	24t, 3ni//4t//2t//4t, 3ni
4.2TAG	261654// 3562566		11t//1//0//0
7.9TAG	262552// 3562714	N90/28S//66	93c//8//0//15

t, theropod footprints; s, sauropod footprints; c, crocodile footprints; ct, crocodile tail traces; ni, unidentified tracks.

Imilchil sites.

2. Location and background

The sites (Table 1) are located (Fig. 1) in the vicinity of Imilchil (Central High Atlas), on the northern flank of the Aït Ali Ou Ikkou Syncline (Charrière and Haddoumi, 2016; Charrière et al., 2011), between the villages of Aït Ali ou Ikkou and Taghighacht (Fig. 1). The coordinates of each of the sites are in Table 1.

The footprints are preserved on sedimentary rocks of the Isli Formation (Charrière et al., 2011). Due to the absence of reliable biomarkers, the precise dating of the base of the formation is uncertain. However, according to the aforementioned authors, this formation would be attributed to the Bathonian?-Callovian interval. According to Klein et al. (2018a), the Isli Formation is fundamentally made up of fluvial sandstones and sandy silts deposited in fluvio-lacustrine environments, probably near the coast. Many of the levels have a brown or even black patina due to weathering ferruginization; apparently unweathered sediments generally have light colors although there may also be scant dark levels of green and grey colors.

We cannot eliminate the influence of reducing environments in the sedimentary basin of the Isli Formation, at least in this area. The Isli Formation extends 57–60 km^2 in the core of the Aït Ali ou Ikkou Syncline, of which we have surveyed about 33 km^2. The sum of the areas of the study surfaces that we analyzed in this work is 4542 m^2. The criterion to consider the area of the sites is subjective, since the line that delimits the environment is drawn surrounding the set of footprints of each site (Fig. 2).

The first paleoichnological publications of Imilchil are from the year 2009 (Gandini, 2009; Gierliński et al., 2009). In chronological order of publication are the citations and descriptions from Gierliński (2016), Gierliński et al. (2017), Klein et al. (2017, 2018a, 2018b, 2022), Oukassou et al. (2019a, 2019b), and finally those of our team (Boutakiout et al., 2020; Masrour et al., 2020, 2021; Minguez Ceniceros et al., 2022). Footprints of dinosaurs (theropods, sauropods and ornithopods), pterosaurs and crocodiles have been have been identified and documented in the previously mentioned studies. These works have contributed new data to the database of vertebrate ichnology. Minguez Ceniceros et al. (2022) elaborated a hypothesis on the spatio-temporal distribution of theropod dinosaurs of especially large size (colossal) and in this work we also present a particular characteristic of the distribution of small and very small dinosaur footprints as an individualized group.

3. Material and method

For the graphic reproduction of footprints and trackways, after cleaning the surface, we used:

i) a reference grid drawn with chalk whose squares (Fig. 2A) have sides of 30 × 30 cm or 60 × 60 cm, depending on the size of the footprints. The direction of the horizontal lines of the grid coincides with the strike of the layer.
ii) If the site only contains one trackway (Fig. 2B), a reference line is drawn along the sequence of footprints.

After that, the outline of the footprints is drawn with chalk and finally the entire surface is photographed. Sometimes a frame with a net of white thread with a mesh size of 5 × 5 cm is placed to better sketch the details of the footprints. Measurements (cf. Leonardi, 1987; Casanovas et al., 1989; Pérez-Lorente, 2015) are taken directly at the site and the entire site is photographed in sections. Photos are first rectified to eliminate any remaining perspective distortion using AdobePhotoshop and drawn using AutoCAD. On this plane (Figs. 3–5) a large part of the measurements are taken and the analysis of the trackways and the associations of footprints as a whole is made. For 3D processing of the images Agisoft Metashape Professional, MeshLab and Paraview software were used.

For the ichnotaxonomic analysis, previous work done in the area (cf. Klein et al., 2022) and the recommendations and limitations (compiled and proposed by Romero-Molina et al., [2003]) of various authors have been considered:

i) on the ichnotaxonomy of dinosaur footprints;
ii) the concepts of theropod footprints (theropod "like" footprints) and footprints of theropod dinosaurs;

We consider (*sensu* Romero-Molina et al., 2003) that all the tridactyl footprints we have found in Imilchil (Figs. 3–5) are theropod footprints (a term not equivalent to footprints of theropod dinosaurs). In general they are longer than wide (Fig. 6) with an oval envelope line (Romero-Molina et al., 2003); tridactyl or tetradactyl, mesaxonic; individualized digits **II-III-IV** directed forwards and with an acuminate termination; more than one pad per digit; angle **II^III** less than **III^IV**; better union between digits **III** and **IV** (in the form of a "V") than between digits **II** and **III**; projecting and rounded heel formed by the metatarsal-phalangeal pad of digit **IV** or bilobed if the proximal pad of digit **II** is printed separately; bipedal gait. We do not work on the length and width of the digits due to the enormous variability of their deformation and the difficulty and disparity of criteria when taking measurements (reference points and their location in the footprint).

There are many papers that have dealt with the reliability of dinosaur tracks when establishing correct ichnotaxonomic criteria (cf. Romero-Molina et al., 2003), and different types of footprints have been defined in relation to their preservation (cf. Diaz-Martínez et al., 2009). In relation to dinosaur footprints whose geometry is a shaft (Allen, 1997), the separation between true footprints and undertracks was established, which over time has been unclear (cf. Pérez-Lorente, 2015). The definition of a true footprint is confusing because it has been used

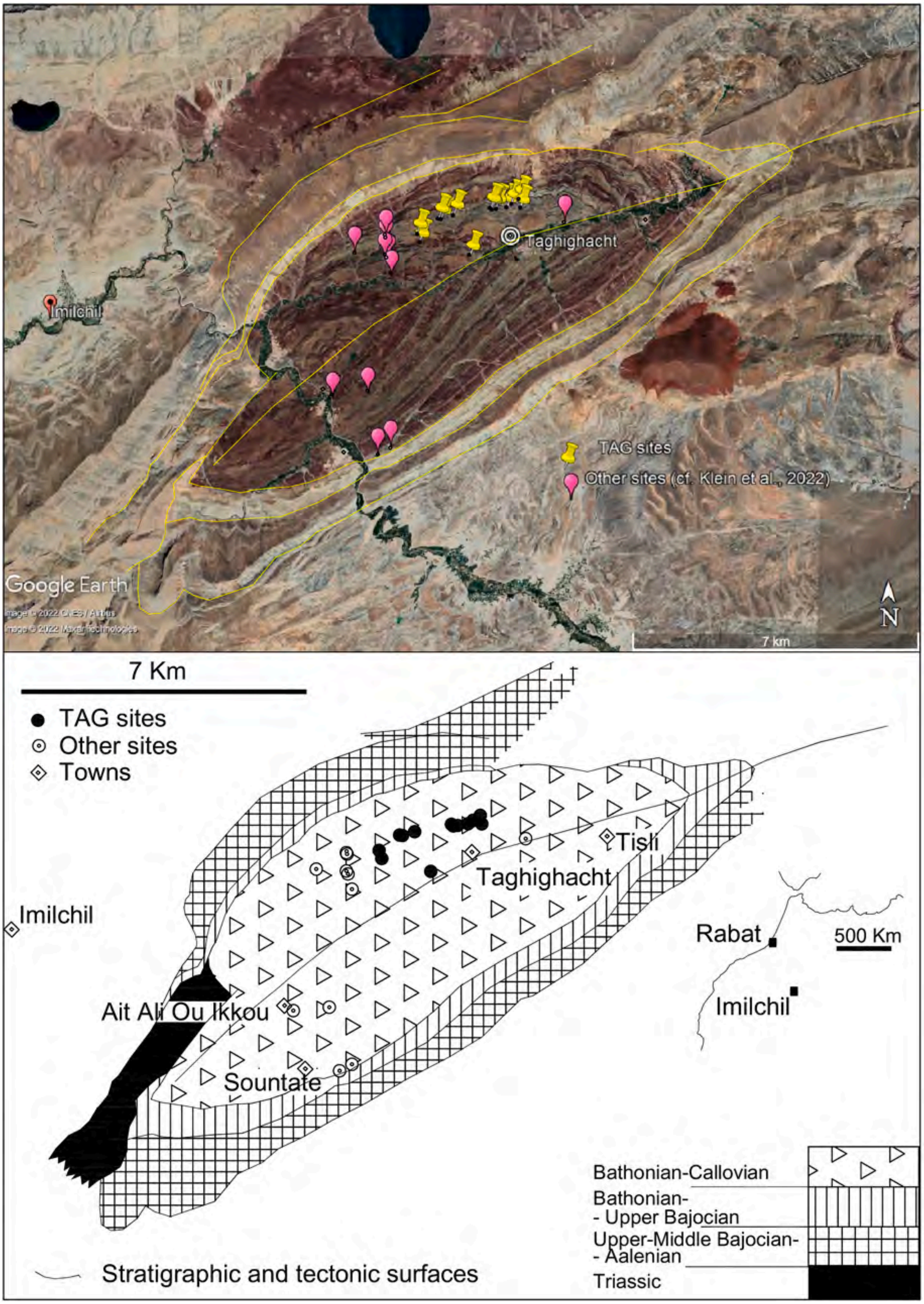

Fig. 1. Location of the sites Above, Geological map of Aït Ali ou Ikkou syncline based on Klein et al. (2022) and their geographical situation. Below, a Google Earth image with the sites described in this work (yellow) and the sites already published by other authors (purple).

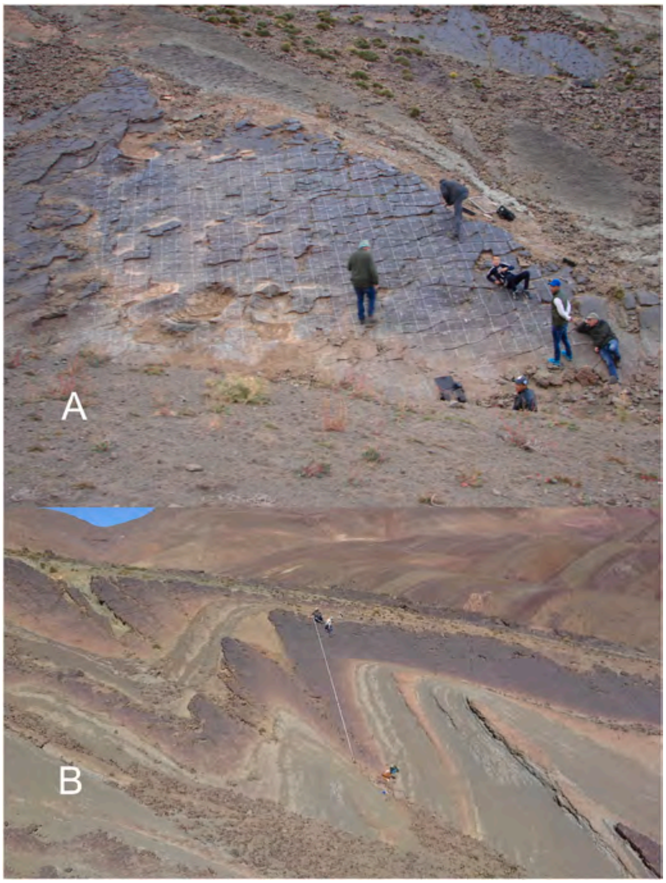

Fig. 2. A, net with chalk on the 7.10TAG site; mesh of 30 × 30 cm. B, reference line on a site (4.2TAG) that contains only a trackwway.

for:

i) footprints (Sarjeant, 1990) "formed in the bedding plane one is examining" (see also Milan and Bromley, 2006; Lockley, 1991),
ii) footprints as undertracks that "do not represent distortions (sensu Peabody, 1955) of the optimal expression of foot morphology" (Lockley and Xing, 2015).

In other words, "true footprints" with optimal representation of the morphology of the foot can be formed below the tracking surface:

i) being direct structures (Gatesy, 2003) or real footprints (Boutakiout et al., 2006; Hadri and Pérez-Lorente, 2012) or
ii) being indirect structures or undertracks (Lockley and Xing, 2015).

In this work we use real footprints for the traces shown by direct structures, deformed or not (Requeta et al., 2006–2007; Pérez-Lorente, 2015). We separate the real footprints into.

i) footprints totally or partially limited by direct structures on or under the tracking surface;
ii) true footprints, deformed or not that remain on the same tracking surface,
iii) Stamps are the real footprints that are the faithful representation of the base of the autopodium (Brown, 1999; Requeta et al. 2006–2007).

Many of the footprints are not real, that is, they are not structures showing the surface with which the autopod skin contacted (direct structures) (Gatesy, 2003). Of course there are very few footprints that we can consider stamps. Many of the Imilchil real footprints are not stamps because they are deformed by direct structures produced by elements of the autopodium itself (eg, dragging of claws), by subsequent movements of the mud, or by interference with other footprints. The bottom of the digit traces may be occupied by a cleft indicating that the digit has crossed it, or that there is closure of the hollow (total or partial) due to the collapse of the walls of the footprint: these structures are called basal striae or basal incisions (Boutakiout et al., 2006) sometimes indistinguishable from claw drag striae. The latter are usually straight.

Sometimes it is easy to distinguish the undertracks from the stamps or the real prints, as in 7.3 TAG (Fig. 7) where the ripples are deformed, but not flaked by the pressure of the feet. This case illustrates the uncertainty that arises if the study surface did not have ripples. We could confuse the study surface with the tracking surface and the undertracks with real footprints.

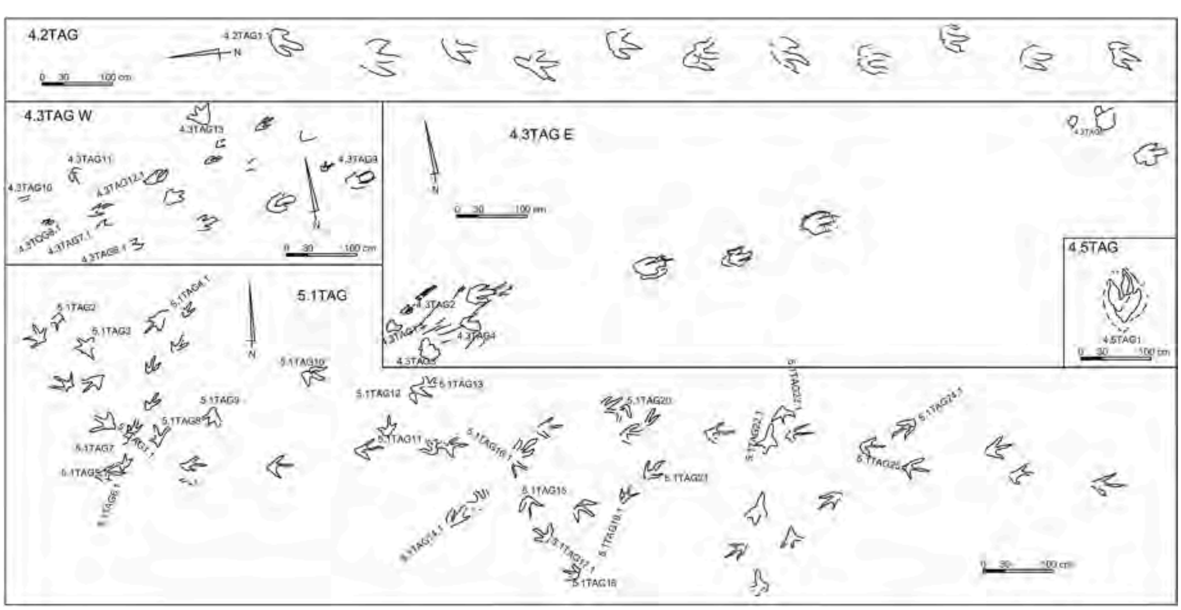

Fig. 3. Footprint cartography of 4.2TAG, 4.3TAG, 4.5TAG and 5.1TAG sites.

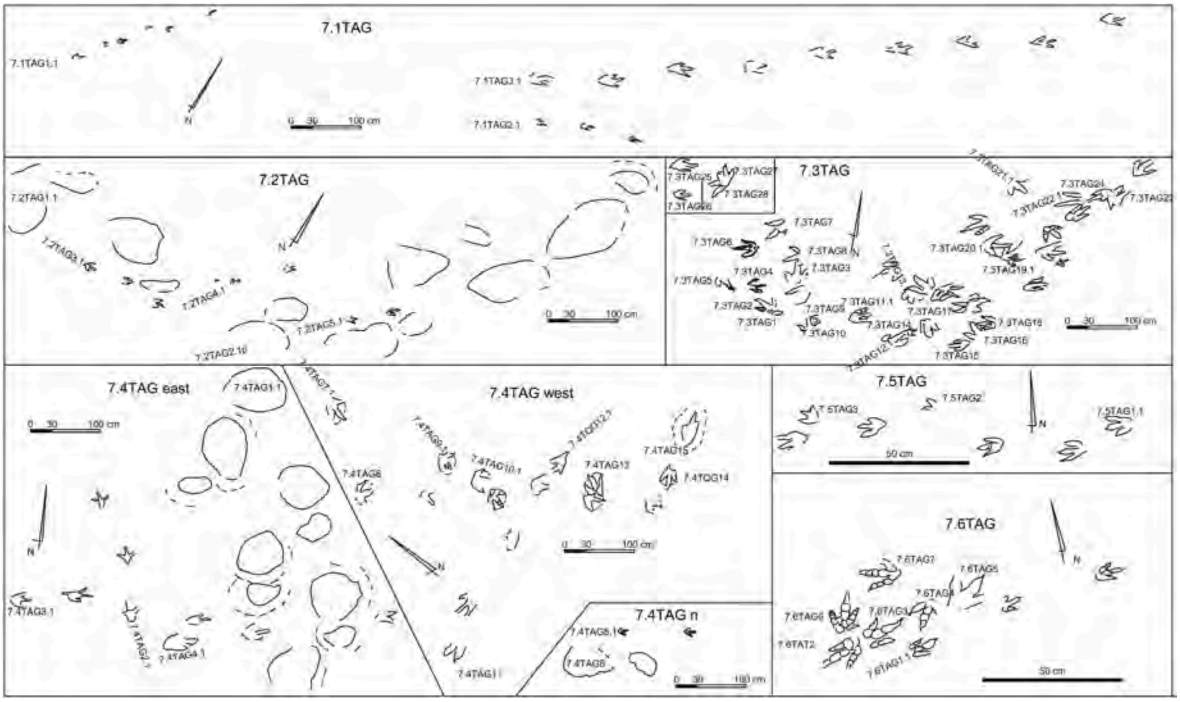

Fig. 4. Footprint cartography of the 7-1TAG, 7.2TAG, 7.3TAG, 7.4TAG, 7.5TAG and 7.6TAG sites.

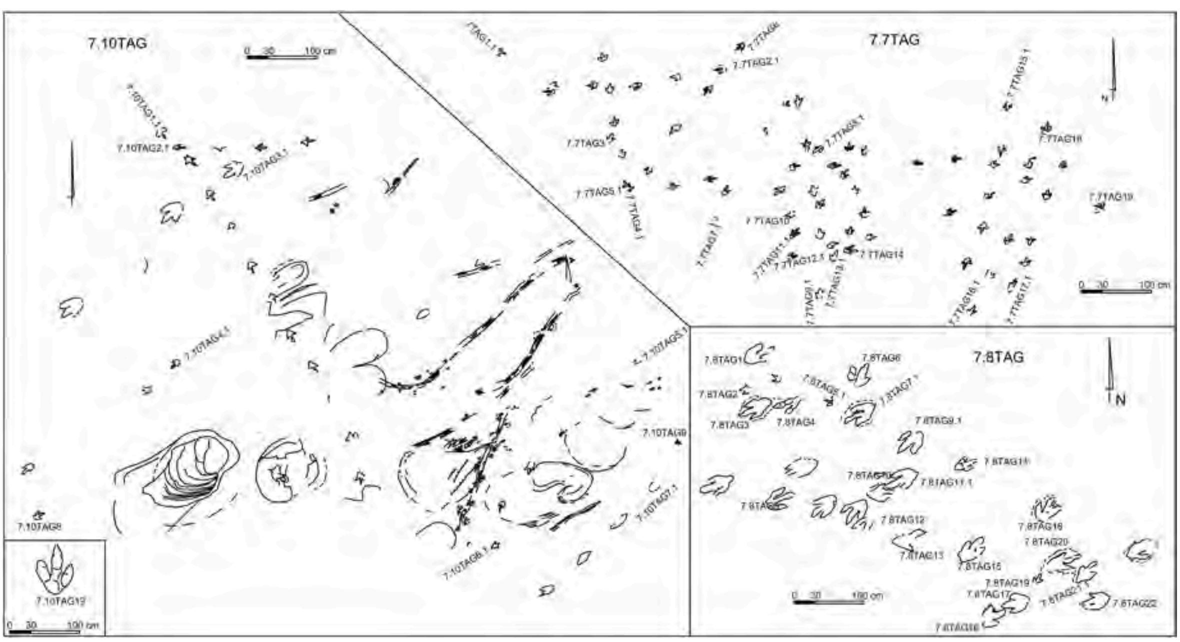

Fig. 5. Footprint cartography of the 7.6TAG, 7.7TAG, 7.8TAG and 7.10TAG sites.

Theoretically, we should know if the footprint surface is a direct structure, but … "Exactly what surface does the dinosaur touch?" (Gatesy, 2003). In Imilchil there are layers with hollows that must correspond to footprints. However, these footprints are currently unrecognizable, and have not been taken into consideration in the present study.

The nomenclature of the footprints (eg 5.1TAG25.2) refers to the site (**5**) of Gandini (2009), to the site number (5.**1**), to the local reference or acronym that we apply to the site (which in this case is **TAG**higacht, 5.1 **TAG**), to the name of the trackway (5.1TAG**25**), and finally to the number of the footprint in the trackway sequence (5.1TAG25.**2**).

The morphometric parameters used by our team (Casanovas et al., 1989) have been traditionally used by researchers from the last century (cf. Casamiquela, 1964; Demathieu, 1970; Haubold, 1971; Leonardi, 1987; Casanovas et al., 1989):

i) **l**, footprint length; **a**, footprint width; **IIˆIIIˆIV** interdigital angles; **te**, projection of digit **III**; **P**, pace length; **z**, stride length; **Ar**, trackway deviation; **Lr**, trackway width; **Ap**, pace angle (pace angulation); **O**, orientation or angle bertween pes axis and midline
ii) and their ratios ([**l**-**a**]/**a**, relative footprint length; **h**, acetabulum height according to Thulborn (1990); **z**/**h**, relative stride; **z**/**l**,

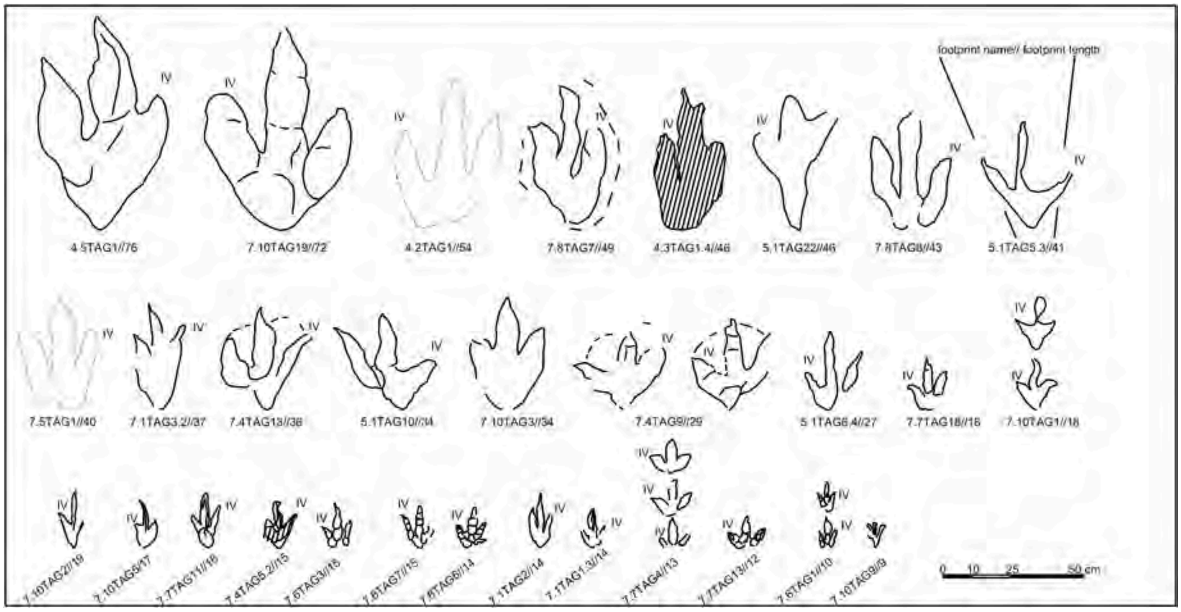

Fig. 6. Representative tridactyl footprints from Imilchil arranged by size. Under the footprints, their identification and their length in cm are indicated.

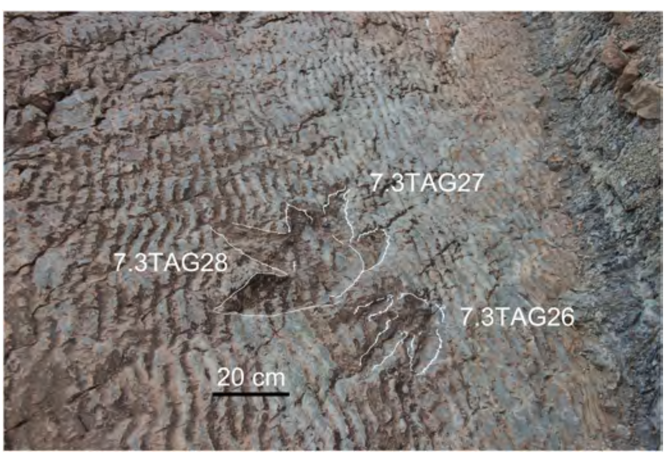

Fig. 7. Deformed ripples in the traces of the 7.3TAG26, 7.3TAG27 and 7.3TAG28 footprints. Ripples and bedding surface predate footprints. The ripples are deformed but not flattened because they are one or more levels below the tracking surface.

Sternberg ratio; **Ar**/**a**, relative trackway deviation; $\mathbf{v_1}$, $\mathbf{v_2}$, walking speed according to Alexander (1976), Demathieu (1986).

The footprint size classification that we adopt comes from several authors:

- colossal (**l** > 70 cm [Minguez Ceniceros et al., 2022])
- giant (**l** > 50 cm [Marty et al., 2017])
- small//large (**l** < 25 cm//**l** > 25 cm [Thulborn, 1990]), and,
- very small (**l** < 15 cm [this work]).

4. Ichnology

In this work, 346 tridactyl footprints from 14 sites are analyzed (Figs. 3–5). At Imilchil we have studied two other sites without tridactyl footprints: 4.1 TAG (sauropod footprints [Boutakiout et al., 2020]) and 7.9 TAG (crocodile footprints [Masrour et al., 2020]). We have also found sauropod footprints (Boutakiout et al., 2020) at 7.2 TAG, 7.4 TAG, and 7.5 TAG (Fig. 4) and sauropod footprints and crocodile tail traces (Masrour et al., 2021) at 7.10 TAG (Figs. 2A and 5). If we suppose that each trackway, each pair of footprints and each isolated footprint (Tables 2 and 3) are from a different dinosaur, the data refer to 138 individuals. If sauropod footprints are also considered, we have found the footrprints of 149 dinosaurs.

The length of the tracks (Fig. 6) ranges (Table 2) between 8 cm (7.6TAG1.2) and 76 cm (4.5TAG1). Footprint length (**l**) is only available for 101 individuals out of the 138 inferred because **l** cannot be measured in all footprints. The width (**a**) of the footprints ranges from 9 cm (9 footprints) to 52 cm (7.10TAG19). The relative width of the footprints ([**l-a**]/**a**) oscillates between the values of −0.3 and 1.7 which implies a wide range between wide footprints to very narrow footprints. Of the 138 possible trackmakers, we have detected 5 with wide footprints and 3 with very narrow footprints (values greater than 1 indicating that the length of the footprint is greater than twice its width).

The shape of the digit traces is apparently very sensitive to changes in the state of the mud. In the 14 Imilchil sites it is difficult to find a tridactyl footprint that does not have acuminate digits and there are very few footprints in which digital pads are discernible. The digits, considered from the hypex, are usually relatively thin and separated. In most of the fopotprints, the asymmetric placement of the digits is very evident:

i) position asymmetry, ia) proximal part of digit **II** advanced, ib) coincidence between the proximal pad of digit **IV** with the heel;
ii) divarication asymmetry, since the value of angle **IIIˆIV** is usually greater than angle **IIˆIII.**

The asymmetry in the position of the digits is the cause of the fact that there is a notch in the back of the foot at its junction with the trace of digit **II**, which, if it is too far back, produces a bilobed shape of the heel (*sensu* Pérez-Lorente, 2001).

4.1. State of the footprints

The state and shape of the footprints, deformed or not, of the sites that we show in this publication are variable. The physical properties of the rocks that form the study surface (Requeta et al., 2006–2007) of each site are found at different sedimentary levels that have behaved and evolved differently. The shape of the footprints in Imilchil fundamentally depends on processes that we separate into three stages:

Table 2
Numerical data of the footprints and trackways.

footprint	l	a	P	z	Ar	Lr	te	IIˆIIIˆIV	Ap	O	NE	h	z/h	z/l	v_1	v_2	(l-a)/a	Ar/a
7.10TAG19	72	52						19–35									0,4	
7.10TAG9	9																	
7.10TAG8	16	12						27–36			N65	72						
7.10TAG7.4			67															
7.10TAG7.3			73	149					179				1.4	6.8	5.3	4.1		
7.10TAG7.2			73	146					180				1.4	6.6	5.1	4.0		
7.10TAG7.1	22	13										103					0.7	
7.10TAG6.2	16		57									72						
7.10TAG6.1	13	10																
7.10TAG5.5	16	9	70									72					0.8	
7.10TAG5.4		11	68	138	2	12			173				1.8	8.1	6.5	4.4		0.2
7.10TAG5.3	16		68	136	2	11			174			72	1.8	8.0	6.4	4.3		0.2
7.10TAG5.2	19		70	142	5	18			162			88	1.8	8.3	6.9	4.5		0.5
7.10TAG5.1																		0.3
7.10TAG4.6	21	12										98						
7.10TAG4.2		11	58															
7.10TAG4.1	16	9										72						
7.10TAG3.4	38	26	106					——25				187					0.5	
7.10TAG3.3			94	196	11	48			153				1.1	5.8	4.2	4.0		0.4
7.10TAG3.2	42	26	106	195	10	44		20–25	157	−3		204	1.1	5.7	4.2	4.0	0.6	0.4
7.10TAG3.1	32	23						7–35				163					0.5	0.4
7.10TAG2.6			84															
7.10TAG2.5	18	12	60	143					175			82	1.7	7.5	6.1	4.3	0.5	
7.10TAG2.4	21	13	69	128					176			98	1.5	6.7	5.1	3.9	0.6	
7.10TAG2.3	16	11	56	125					187			72	1.4	6.6	4.9	3.8	0.4	
7.10TAG2.2			61	117					180				1.4	6.1	4.4	3.5		
7.10TAG2.1	20	9										93					0.7	
7.10TAG1.11	17		55									77						
7.10TAG1.10			63	117					161				1.3	6.5	4	3.5		
7.10TAG1.9			56	119					178				1.4	6.6	4	3.6		
7.10TAG1.8			53	109					193				1.3	6.0	3.5	3.3		
7.10TAG1.7	18	14	57	113	3	18			169			82	1.3	6.3	3,8	3.4	0,3	0.2
7.10TAG1.6	14		56	115	3	17			169			62	1.3	6.4	3.9	3.5		0,2
7.10TAG1.5	19	15	63	119	3	16			169			88	1.4	6.6	4	3.6	0.3	0.2
7.10TAG1.4			58	120	3	16			168				1.4	6.7	4.1	3.6		0.2
7.10TAG1.3	19	14	56	114	1	16			175			88	1.3	6.3	3.8	3.5	0.4	0.2
7.10TAG1.2	22	16	57	112	4	24			165			103	1.3	6,2	3.7	3.4	0.4	0.3
7.10TAG1.1		17															0.3	
7.8TAG22	40	25									————	198					0.6	
7.8TAG21.2			81															
7.8TAG21.1	42	22										204					0.9	
7.8TAG20	52	24									——	247					1.2	
7.8TAG19	19?	12					7	24–29			N29	88					0.6	

(continued on next page)

Table 2 (*continued*)

footprint	l	a	P	z	Ar	Lr	te	II^III^IV	Ap	O	NE	h	z/h	z/l	v_1	v_2	(l-a)/a	Ar/a
7.8TAG18	40	30					14	9–25			N32	198					0.3	
7.8TAG17	44	28					11	14–29			N249	214					0.6	
7.8TAG16	39	28					15	25–33			N79	193					0.4	
7.8TAG15	45	26					12	14–15			N45	218					0.7	
7.8TAG14	38	21						5–24			N68	187					0.8	
7.8TAG13	51											243						
7.8TAG12																		
7.8TAG11.2	43	31	85					6–14				210					0.4	
7.8TAG11.1	51	28					17	2–12				243					0.7	
7.8TAG10																		
7.8TAG9.2	43	26	150				9	10–26				210					0.6	
7.8TAG9.1	45	31					16	13–16				218					0.4	
7.8TAG8	43	28						2–22			N67	210					0.5	
7.8TAG7.3	51	28	124									243					0.8	
7.8TAG7.2			116	230	17	43			148				0.9	4.7	4.1	4.2		
7.8TAG7.1	48	27					16	10–21				231					0.8	
7.8TAG6	39	32					16	8–35			N27	172					0.2	
7.8TAG5.2	15		83					——33				67						
7.8TAG5.1	15?	16?						40——				67						
7.8TAG4											N250							
7.8TAG3	50	25									N241	239					1	
7.8TAG2		14																
7.8TAG1	46	27					16	6–27			N64	223					0.7	
7.7TAG19		13						16–20			N209							
7.7TAG18	18	13						9–26			N21	82					0.4	
7.7TAG17.5	15	13					6	12–36				67					0.1	
7.7TAG17.3		13	32	69	3	18		25–74					1.1	4.9	2.7	3.0		
7.7TAG17.2	14	14	40	70			5	45–28	159	−4		62	1.1	5.0	2.7	3.0	0	
7.7TAG17.1		5					4											
7.7TAG16.5		12																
				114									1.5	6.7	4.8	3.6		
7.7TAG16.3	17	12	57		0			——23				77					0.4	
7.7TAG16.2			54						180									
7.7TAG16.1		13																
7.7TAG15.5	18	13	54				8	28–19				82	1.3				0.4	
7.7TAG15.4	17	16					7	24–37				77	1.6				0.1	
				113										6.3	4.5	3.5		
7.7TAG15.2	18	13	64				9	36–54				82	1.3				0.4	
7.7TAG15.1		12					5	54–33										
7.7TAG14	20	12					7	22–32			N91	93					0.6	
7.7TAG13.6	12	13										52					−0.1	

(*continued on next page*)

Table 2 (*continued*)

footprint	l	a	P	z	Ar	Lr	te	IIˆIIIˆIV	Ap	O	NE	h	z/h	z/l	v_1	v_2	(l-a)/a	Ar/a
7.7TAG13.4																		
7.7TAG13.3																		
7.7TAG13.2	11	12										47					−0.1	
7.7TAG13.1																		
7.7TAG12.8		10	59					14–26										
7.7TAG12.7	18	9	55	116	1	10		19–21	176	7		82	1.5	6.8	5.0	3.7	1	
7.7TAG12.6	17		62	117	0			——20	180	0		77	1.5	6.9	5.1	3.8		
7.7TAG12.5	20	10						19–14				93					1	
————				115									1.5	6.7	5.0	3.7		
7.7TAG12.3	15	9	57					17–36				67					0.7	
7.7TAG12.2	17		57	111								77	1.5	6.5	4.7	3.6		
7.7TAG12.1	15							19				67						
7.7TAG11.4	13		45					——40				57						
7.7TAG11.3	15	11	56	102	1		7	9–24	176	9		67	1.4	6.4	4.3	3.4	0.4	
7.7TAG11.2	16	11	57	113	1	12	6	38–22	177	−1		72	1.6	7.1	5.1	3.7	0.4	
7.7TAG11.1	20	11					6	32–15				93					0.8	
7.7TAG10											N259							
7.7TAG9.5	>16		63					19——										
7.7TAG9.4	>16	13	68	132	2	17		22–58	174	−1		67	1.9	8.2	6.8	4.4		
7.7TAG9.3	15		68	129	1				177				1.8	8.1	6.5	4.3		
7.7TAG9.2	14		81	143	4	20		——38	170	3			2.0	8.9	7.8	4.8		
7.7TAG9.1	16											72						
7.7TAG8.2	20	12	81				8	19–33				93					0.7	
7.7TAG8.1	18	10					8	9–24				82					0.8	
7.7TAG7.6			51															
7.7TAG7.5																		
————																		
————																		
7.7TAG7.2	16		44															
7.7TAG7.1																		
7.7TAG6.4			73					20——										
7.7TAG6.3	18	10	73	145	2	16						82	1.8	8.5	7.0	4.6	0.8	
7.7TAG6.2	17	11	76	149		14		——36	179	0		77	1.9	8,8	7.3	4.7	0.7	
7.7TAG6.1	17	10					10	16–21				77					0.7	
7.7TAG5.11			58															
7.7TAG5.10	17		57	115	4	17		15——	165	−4		77	1.7	7.2	5.6	3.9		
7.7TAG5.9	14	10	51	108	3			11–36	165	4		62	1.6	6.7	5.0	3.7	0.4	
7.7TAG5.8	15							22——				67						
————				121									1.8	7.6	6.1	4.1		
7.7TAG5.6																		
7.7TAG5.5			60					5——										
————																		
7.7TAG5.3		9	53					17–15										
7.7TAG5.2		10	60	112	2	15		8–25	172	2			1.6	7	5.3	3.8		
7.7TAG5.1		9						26–32										
7.7TAG4.5	12	14					6	43–28				52					−0.1	
7.7TAG4.4	13	12	47	94	1	16		——42	176	10		57	1.7	7.2	5.0	3.5	0.1	
7.7TAG4.3	13	14	47	95	1	16	5	26–35	173	5		57	1.7	7.3	5.1	3.5	−0.1	
7.7TAG4.2	13		47	95	1	15			173	12		57	1.7	7.3	5.1	3.5		
7.7TAG4.1		11					6	38–40										

(*continued on next page*)

Table 2 (*continued*)

footprint	l	a	P	z	Ar	Lr	te	IIˆIIIˆIV	Ap	O	NE	h	z/h	z/l	v_1	v_2	(l-a)/a	Ar/a
7.7TAG3		11									N27							
7.7TAG2.5	18	11	60									82					0.6	
7.7TAG2.4	16	11	63	123	2	16		25–50	174	10		72	1.5	6.8	5.1	3.8	0.4	
7.7TAG2.3	19	11	63	119	3			——30	169	8		88	1.5	6.6	4.8	3.7	0.7	
7.7TAG2.2	18		66	123	1				178	6		82	1.5	6.8	5.1	3.8		
7.7TAG2.1	18	12										82					0.5	
7.7TAG1.2																		
7.7TAG1.1																		
7.6TAG7	15	11						15–46			N103	67					0.4	
7.6TAG6	14	10						17–31			N18	62					0.4	
7.6TAG5											N77							
7.6TAG4	12										N212	52						
7.6TAG3	15	11						11–25			N73	57					0.4	
7.6TAG2	18?	10						3–36			N255	82					0.8	
7.6TAG1.3	11	6	36				4.2	7–23				47					0.8	
7.6TAG1.2	8	5	36	72	1.6	9	3.9	24—	170	7		32	1.7	7.2	4.5	3.1	0.6	
7.6TAG1.1	11	6					4.7	28–21				47					0.8	
7.5TAG3	28	28									N298	137					0	
7.5TAG2																		
7.5TAG1.6	44		115					15——				214						
7.5TAG1.5	41	28						3–26				202					0.5	
——————				174									0.9	4.3	3.1	3.4		
7.5TAG1.3	37	27	124					——24				185					0.4	
7.5TAG1.2	40	30	76	184	15	52		17–27	149	−5		198	0.9	4.6	3.5	3.6	0.3	
7.5TAG1.1	40	34						14–21				198					0.2	
7.4TAG15																		
7.4TAG14	29	25						26–39			N241	145					0.2	
7.4TAG13	36	32						9–32			N20	180					0.1	
7.4TAG12.3			131															
7.4TAG12.2			109	240					180									
7.4TAG12.1																		
7.4TAG11																		
7.4TAG10.4			88					15——										
7.4TAG10.3	32		76	164	3			——39	170	9		163	1.0	5.1	3.6	3.6		
7.4TAG10.2		34	85	161					171									
7.4TAG10.1													1.0	5.0	3.6	3.5		
7.4TAG9.2	32	30	84					21–38				163					0.1	
7.4TAG9.1	26	33						18——				128					−0.2	
7.4TAG8	28											137						
7.4TAG7.2			183															
7.4TAG7.1																		
7.4TAG5.2	14		94					3–40				62	1.3					
7.4TAG5.1	17	12						33—				77					0.4	
7.4TAG4.4																		

(*continued on next page*)

Table 2 (*continued*)

footprint	l	a	P	z	Ar	Lr	te	IIˆIIIˆIV	Ap	O	NE	h	z/h	z/l	v_1	v_2	(l-a)/a	Ar/a
———————				194									1.0	4.3	3.6	3.8		
7.4TAG4.2	39	24	113									193					0.6	
7.4TAG4.1	51	21										243					1.4	
7.4TAG3.4	36	14						——22				180					1.5	
———————				178									1.1	5.7	3.1	3.9		
7.4TAG3.2	36	21	80					17–25				180					0.7	
7.4TAG3.1	29	22						26——				141					0.3	
7.4TAG2.3			89					75–57										
7.4TAG2.2	24		82	167	7	26		55–73	159	0		115	1.4	7.0	5.6	4.4		
7.4TAG2.1																		
7.3TAG22.4			138															
7.3TAG22.3		29	142	278	11				164				2.0	6.0	6.1	5.2		
7.3TAG22.2	46	29	140	279	10			17–24	164	0		223	2.0	6.1	6.1	5.2	0.6	
7.3TAG22.1								18——										
7.3TAG21.2			87					20–53										
7.3TAG21.1	28	30						50				137					−0.1	
7.3TAG20.2	43	27	82					15–37				210					0.6	
7.3TAG20.1	41	32						35–31				202					0.3	
7.3TAG19.2	19	11	70					32–48				88					0.1	
7.3TAG19.1																		
7.3TAG18	28	18						4–28			N260	137					0.5	
7.3TAG17											———							
7.3TAG16.2	35	32	102					7–39				176					0.1	
7.3TAG16.1								——38										
7.3TAG15		16						1–29			N251							
7.3TAG14	15?	11?									———							
7.3TAG13.2	28	28	51					1–26				137					0	
7.3TAG13.1																		
7.3TAG12.5			113					23–25										
7.3TAG12.4		19	110	224	0	17		1–13	180									
7.3TAG12.3			116	225	1	18		27——	180									
7.3TAG12.2		20	95	210	6	33		7–38	168	−11								
7.3TAG12.1								11–34										
7.3TAG11.3		17	119					12–7										
7.3TAG11.2			137	254	8	31		32–16	165	−4			1.5	7.4	7.0	5.4		
7.3TAG11.1	34	21						16–5				172					0.6	
7.3TAG10											———							
7.3TAG9											———							
7.3TAG8											N245							
7.3TAG7								———31			N219							
7.3TAG6	35	26						13–25			N256	176					0.7	
7.3TAG5											N235							
7.3TAG4		21						23–35			N73							
7.3TAG3											N245							

(*continued on next page*)

Table 2 (*continued*)

footprint	l	a	P	z	Ar	Lr	te	II˄III˄IV	Ap	O	NE	h	z/h	z/l	v_1	v_2	(l-a)/a	Ar/a
7.3TAG2								21–48			N294							
7.3TAG1											——							
7.2TAG5.2	18	11	60					16–32				82					0.6	
7.2TAG5.1								26 –										
7.2TAG4.5																		
7.2TAG4.2																		
7.2TAG4.1																		
7.2TAG3.3			53										0.6					
7.2TAG3.2			56	109	3				166				0.6	5.7	3.7	3.2		
7.2TAG3.1	19	13						23–47				88					0.5	
7.1TAG3.9			105															
7.1TAG3.8			112	212	8	36		21–25	162	−2			1.1	5.7	4.8	4.3		
7.1TAG3.7		21	94	203	4	22			171				1.1	5.5	4.4	4.2		
7.1TAG3.6			113	207	2	21			176				1.1	5.6	4.6	4.2		
7.1TAG3.5			101	213	4	27			172				1.1	5.7	4.8	4.4		
7.1TAG3.4			108	207	4	37			170				1.1	5.6	4.6	4.2		
7.1TAG3.3	38	16	100	201	4	25		16–30	171	−10		187	1.1	5.4	4.3	4.1	1.4	
7.1TAG3.2	37	18	106	205	5			2–23	163	−4		185	1.1	5.5	4.5	4.2	1.5	
7.1TAG3.1																		
7.1TAG2.3	10		76					—26				42						
7.1TAG2.2	19		68	139	3			26—	170	0		88	2.1	9.9	8.1	4.8		
7.1TAG2.1		9						15–23										
7.1TAG1.7																		
				65			6	—43					1	4.6	2.2	2.3		
7.1TAG1.5			30										4					
7.1TAG1.4			33	66				19–34	151				1	4.6	2.3	2.3		
7.1TAG1.3	14	9	26	64					162	0		62	1	4.6	2.2	2.3	0.5	
7.1TAG1.2			40	66					165				1	4.6	2.3	2.3		
7.1TAG1.1		17						29—										
5.1TAG25.3	49	31	155					30–37										
5.1TAG25.2		32	115	266	2		18	14–51		−1								
5.1TAG25.1	41	30						27–60										
5.1TAG24.3	37	23	153				15	1–39										
5.1TAG24.2	42	25	147	297	12	45	14	7–42	163	−5								
5.1TAG24.1	43	25						11–25										
5.1TAG23.3																		
5.1TAG23.2				176														
5.1TAG23.1																		
5.1TAG22.3			107															
5.1TAG22.2	48		103	210	3			29–38	173	10								
5.1TAG22.1	44	33						——60										
5.1TAG21	38	29					16	36–45			N49	187					0.2	
5.1TAG20											——							
5.1TAG19.2			106					20——										
5.1TAG19.1	37	23						5–46				185					0.6	
5.1TAG18	24										N289	115						

(*continued on next page*)

Table 2 (*continued*)

footprint	l	a	P	z	Ar	Lr	te	IIˆIIIˆIV	Ap	O	NE	h	z/h	z/l	v_1	v_2	(l-a)/a	Ar/a
5.1TAG17.3			102					22–49										
5.1TAG17.2			103	202	10	51	10	15————					1.4	7.2	6.3	4.8	−0.2	0.3
5.1TAG17.1	28	34						38–59	159	−13		137						
5.1TAG16.2	29	36	119				10	25–41				141					−02	
5.1TAG16.1								46										
5.1TAG15	32	35					11	29–59			N186	163					−0.1	
5.1TAG14.3			140					1–42										
5.1TAG14.2		25	132	268	11	48	16	19–25	168	0								
5.1TAG14.1								29–59										
5.1TAG13																		
5.1TAG12	34							21–45			N119	172						
5.1TAG11	29	26						32–60			N0	141					0.1	
5.1TAG10	34	36						28–34			N122	172					−0.2	
5.1TAG9.2			99															
5.1TAG9.1																		
5.1TAG8	32										N356	163						
5.1TAG7																		
5.1TAG6.6	32		52					16——				163						
5.1TAG6.5		23	48		7	35		29–30	146	1								
5.1TAG6.4	28	20	50	95	10	42	10	14–30	130	8		137	0.7	3.5	1.9	2.3	0,4	
5.1TAG6.3	29	19	46	88	7	36	9	——29	144	15		141	0.7	3.2	1.6	2.1	0.5	
5.1TAG6.2		20	52	91	4	28		24–18	159	4			0.7	3.4	1.7	2.2		
5.1TAG6.1	24			96			9	23——				115	0.7	3.5	1.9	2.3		
5.1TAG5.11	50	31	178				13	35–35				239					0.6	
5.1TAG5.10	36	29	165	286	3	20	15	26–44	174	0		180	1.2	7.0	6.2	5.2	0.2	
5.1TAG5.9	41		115	223	4	34		——19	173	5		202	1.0	5.4	4.1	3.4		
5.1TAG5.8	42	30	127	240	1			45–34	179	6		204	1.0	5.8	4.6	4.4	0.4	
5.1TAG5.7		29	118	243	2	35		28–45	176	0			1.1	5.9	4.7	4.5		
5.1TAG5.6	37	30	135	253	8	16		43–29	165	4		185	1.1	6.2	5.1	4.7	0.2	
5.1TAG5.5	45	28	128	261	5	40	15		170			218	1.1	6.4	5.3	4.8	0.6	
5.1TAG5.4	41	29	127	252	5	39	15	33–33	171	−2		202	1.1	6.1	5.1	4.7	0.4	
5.1TAG5.3	38	32	123	250	6	42	16	38–47	168	8		187	1.1	6.1	5.0	4.6	0.2	
5.1TAG5.2	39		117	243	4	48	13	19–36	172	6		193	1.1	5.9	4.7	4.5		
5.1TAG5.1								31——										
5.1TAG4.2	37	22	121									185					0.7	
5.1TAG4.1	45	22										218					1.0	
5.1TAG3	38	32									N318	187					0.2	
5.1TAG2	24										N179	115						
5.1TAG1.3	30	40	77					62–46				145					−0.2	
5.1TAG1.2	31	57	83	160	4	47		60–19	167	21		159	1.0	6.0	3.8	3.6	−0.5	
5.1TAG1.1		39						51–35										
4.5TAG1	76	46																
4.3TAG13	31	36									N337	159						
4.3TAG12.2	15		95									67						
4.3TAG12.1																		

(*continued on next page*)

Table 2 (*continued*)

footprint	l	a	P	z	Ar	Lr	te	IIˆIIIˆIV	Ap	O	NE	h	z/h	z/l	v_1	v_2	(l-a)/a	Ar/a
4.3TAG11	—	—	—	—	—	—	—	—	—	—	—	—	—	—	—	—	—	—
4.3TAG10	—	—	—	—	—	—	—	—	—	—	—	—	—	—	—	—	—	—
4.3TAG9	—	—	—	—	—	—	—	—	—	—	—	—	—	—	—	—	—	—
4.3TAG8.5	31	12	84		6	25		13	162	3		159					1.6	
4.3TAG8.4		11	91	173	5	24			168				1.1	5.7	4.3	3.9		
4.3TAG8.3	30	45	95	184	5	25		16–24	167	−2		145	1.2	6.1	4.8	4.2	−0.3	
4.3TAG8.2			76	170									1.1	5.7	4.2	3.9		
4.3TAG8.1	—	—	—	—	—	—	—	—	—	—	—	—	—	—	—	—	—	—
4.3TAG7.4			93															
4.3TAG7.3			119	212					175				1.3	6.8	5.7	4.7		
4.3TAG7.2	31	20	110	229					178			159	1.4	7.4	6,5	5.1	0.5	
4.3TAG7.1	—	—	—	—	—	—	—	—	—	—	—	—	—	—	—	—	—	—
4.3TAG6.4	48?		120									231						
4.3TAG6.3	42	25	117	238	0	25			180	0		204	1	5.3	4.8	4.5	0.7	
4.3TAG6.2	—	23	104	222	0	27	—	6–18	180	—	—	—	1	4.9	4.3	4.2	—	—
4.3TAG6.1	—	—	—	—	—	—	—	—	—	—	—	—	—	—	—	—	—	—
4.3TAG5.2	—	—	—	—	—	—	—	—	—	—	—	—	—	—	—	—	—	—
4.3TAG5.1	—	—	—	—	—	—	—	—	—	—	—	—	—	—	—	—	—	—
4.3TAG4	—	—	—	—	—	—	—	—	—	—	—	—	—	—	—	—	—	—
4.3TAG3	—	—	—	—	—	—	—	—	—	—	—	—	—	—	—	—	—	—
4.3TAG2	—	—	—	—	—	—	—	—	—	—	—	—	—	—	—	—	—	—
4.3TAG1.11	50	30						11———				239					0.7	
4.3TAG1.6	52?	29	118					—11				247					0.8	
4.3TAG1.5	36	23	137	250	11	46		5—	160	−9		180	1	6.5	4.8	4.9	0.6	
4.3TAG1.4	51	24						6–10				243				4.9	1.1	
				249									1	6.5	4.7			
4.3TAG1.2	41	28	129					1–12				202					0.5	
4.3TAG1.1	—	—	—	—	—	—	—	—	—	—	—	—	—	—	—	—	—	—
4.2TAG1.11	51	33	128					13–25				243					0.5	
4.2TAG1.10	47	33	116	242	8	50		———20	165	−11		226	0.9	4.5	4.1	4.2	0.4	
4.2TAG1.9	51	44	124	233	15	67	13	19——	152	0		243	0.9	4.3	3.8	4.1	0.2	
4.2TAG1.8	46	36	117	238	10	61		——24	161	1		223	0.9	4.4	4.0	4.2	0.3	
4.2TAG1.7	64	39	123	240	3	49	18	11–3	173	−19		294	0.9	4.4	4.1	4.2	0.6	
4.2TAG1.6			117	238	8	52		8–22	165	−8			0.9	4.4	4.0	4.2		
4.2TAG1.5			120	229	14	66		15–41	152	−6			0.9	4.2	3.8	4.0		
4.2TAG1.4	56		122	234	15	71		——39	150	1		263	0.9	4.5	3.8	4.1		
4.2TAG1.3	69?	40	116	233	12			22——	157	−1		314	0.9	4.3	3.8	4.1	0.7	
4.2TAG1.2		49	141	252	12	62		21–22	158	−4			1	4.7	4.4	4.4		
4.2TAG1.1	49	36					21	14–14		−4		235					0.4	

Measurements in cm and sexagesimal degres.

Table 3
Numerical data of isolated footprints and average data of pairs of footprints and trackways.

Trackways, pairs and isolated footprints	l	a	P	z	Ar	Lr	te	IIˆIIIˆIV	Ap	O	h	z/h	z/l	v_1	v_2	(l-a)/a	Ar/a
7.10TAG 19	72	52						19–35								0.4	
7.10TAG9	9																
7.10TAG8	16	12														0.3	
7.10TAG7	22	13	71	147					180		103	1.4	6.7			0.7	
7.10TAG6	14	10														0,4	
7.10TAG5	17	10	69	139	3	14			170		77	1.8	8.1			0.8	0.3
7.10TAG4	18	10	58								85					0.8	
7.10TAG3	34	25	102	196	10	46		13–27	155	−3	184	1.1	5.7			0.4	0.4
7.10TAG2	19	11	66	128					180		86	1.5	6.7	4.2	4.0	0.6	
7.10TAG1	18	15	57	115	3	18			172		85	1.3	6.4	3.9	3.5	0.3	0.2
7.8TAG22	40	25									198					0.6	
7.8TAG21	42	22	81								204						
7.8TAG20	52	24									247					1.2	
7.8TAG19	19?	12					7	24–29			88					0.6	
7.8TAG18	40	30					14	9–25			198					0.3	
7.8TAG17	44	28					11	14–29			214					0.6	
7.8TAG16	39	28					15	25–33			193					0.4	
7.8TAG15	45	26					12	14–15			218					0.7	
7.8TAG14	38	21						5–24			187					0.8	
7.8TAG13	51										243						
7.8TAG12																	
7.8TAG11	47	30	85				17	4–13			226					0.5	
7.8TAG10																	
7.8TAG9	44	28	150				12	12–21			214					0.5	
7.8TAG8	43	28						2–22			210					0.5	
7.8TAG7	49	27	120	230	17	43	16	10–21	148		237	0.9	4.7	4.1	4.2	0.8	0,4
7.8TAG6	39	32					16	8–35			172					0.2	
7.8TAG5	15	16	83					40–33			67						
7.8TAG4																	
7.8TAG3	50	25									239					1	
7.8TAG2		14															
7.8TAG1	46	27					16	6–27			223					0.7	
7.7TAG19		13						16–20									
7.7TAG18	18	13					7	9–26			82					0.4	
7.7TAG17	14	11	36	70	3	18	5	35–51	159	−4	62	1.1	5.0	2.7	3.0	0	0.3
7.7TAG16	17	13	55	114	0			——23	180		77	1.5	6.7	4.8	3.6	0.4	0
7.7TAG15	18	13	59	113			7	35–36			80	1.4	6.3	4.5	3.5	0.3	
7.7TAG14	20	12					7	22–32			93					0.6	
7.7TAG13	12	12									50					−0.1	
7.7TAG12	17	10	58	115	1	10		18–23	178	3	75	1.5	6.7	5.0	3.7	0.9	0.0
7.7TAG11	16	11	52	107	1	12	6	26–25	176	4	72	1.5	6.7	4.7	3.5	0.5	0.1
7.7TAG10																	
7.7TAG9	16	13	70	134	2	18		20–48	174	1	70	1.9	8.4	6.7	4.5	0.3	0.1
7.7TAG8	19	11	81				8	14–28			87					0.7	
7.7TAG7			44														
7.7TAG6	17	10	74	146	2	15	10	18–28	179	0	78	1.9	8.6	7.1	4.6	0.7	0.2
7.7TAG5	16	9	56	114	3	16		15–27	167	0	68	1.7	7.1	5.5	3.6	0.4	0.3
7.7TAG4	13	13	47	95	1	16	6	36–34	174	9	56	1.7	7.3	5.1	3.5	−0.0	0.1
7.7TAG3		11															
7.7TAG2	18	11	64	122	2	16		25–40	173	8	81	1.5	6.7	5.0	3.8	0.5	0.2
7.7TAG1																	
7.6TAG7	15	11						15–46			67					0.4	
7.6TAG6	14	10						17–31			62					0.4	
7.6TAG5																	
7.6TAG4	12										52						
7.6TAG3	15	11						11–25			57					0.4	
7.6TAG2	18?	10						3–36			82					0.8	
7.6TAG1	10	6	36	72	2	9	4	19–22	170	7	42	1.7	7.2	4.5	3.1	0.7	0.3
7.5TAG3	28	28									137					0	
7.5TAG2																	
7.5TAG1	40	30	105	177	13	52		12–24	149	−5	199	0.9	4.5	3.3	3.4	0.3	0.5
7.4TAG15																	
7.4TAG14	29	25						23–39			145					0.2	
7.4TAG13	36	32						9–32			180					0.1	
7.4TAG12			120	240					180								
7.4TAG11																	
7.4TAG10	32	34	83	162	3			15–39	170	9	163	1.0	5.0	3.6	3.6	- 0.1	0.05
7.4TAG9	29	31	84					20–38			145					0	
7.4TAG8	28										137						
7.4TAG7			183														
7.4TAG5	15	12	94					18–40			70	1.3				0.4	
7.4TAG4	45	22	113	194							206	0.9	4.3	3.6	3.8	1.1	
7.4TAG3	31	16	80	178				21–23			167	1.1	5.7	3.1	3.9	0.8	
7.4TAG2	24		85	167	7	26		65–65	159	0	115	1.4	7.0	5.6	4.4		

(*continued on next page*)

Table 3 (*continued*)

Trackways, pairs and isolated footprints	l	a	P	z	Ar	Lr	te	IIˆIIIˆIV	Ap	O	h	z/h	z/l	v_1	v_2	(l-a)/a	Ar/a
7.3TAG24																	
7.3TAG23																	
7.3TAG22	46	29	140	278	10			17–24	164	0	223	2.0	6.0	6.1	5.2	0.6	0.5
7.3TAG21	28	30	87					35–53			137					−0.1	
7.3TAG20	42	30	82					25–34			206					0.4	
7.3TAG19	19	11	70					32–38			88					0.1	
7.3TAG18	28	18						4–28			137					0.5	
7.3TAG17																	
7.3TAG16	35	32	102					7–38			176					0.1	
7.3TAG15		16						1–29									
7.3TAG14	15?	11?															
7.3TAG13	28	28	51					1–26			137					0	
7.3TAG12		19	108	220	2	22		14–27	176	−11							0.5
7.3TAG11	34	19	128	254	8	31		20–9	165	−4	172	1.5	7.4	7.0	5.4	0.6	0.4
7.3TAG10																	
7.3TAG9																	
7.3TAG8																	
7.3TAG7								———31									
7.3TAG6	35	26						13–25			176					0.7	
7.3TAG5																	
7.3TAG4		21						23–35									
7.3TAG3																	
7.3TAG2								21–48									
7.3TAG1																	
7.2TAG5	18	11	60					21–32			82					0.6	
7.2TAG4																	
7.2TAG3	19	13	55	109	3			23–47	166		88	0.6	5.7	3.7	3.2	0.5	0.2
7.1TAG1	14	13	35	65			6	24–38	159	0	62	1	4.6	2.2	2.3	0.3	
7.1TAG2	14	9	72	139	3			20–24	170	0	65	2.1	9.9	8.1	4.8	0.7	0.3
7.1TAG3	37	18	106	207	4	28		19–26	170	−5	186	1.1	5.6	4.6	4.2	1.4	0.2
5.1TAG25	45	33	133	266	2		18	25–49	163	−5	216	1.2	6	5.8	5.1	0.3	0.06
5.1TAG24	41	24	150	297	12	36	14	6–35	163	−5	200	1.5	7.3	7.7	5.9	0.7	0.5
5.1TAG23				176													
5.1TAG22	46	33	105	210	3			29–49	173	10							0.09
5.1TAG21	38	29					16	36–45			187					0.2	
5.1TAG20																	
5.1TAG19	37	23	106					12–46			185					0.6	
5.1TAG18	24										115						
5.1TAG17	28	34	103	202	10	51	10	25–54	159	−13	137	1.4	7.2	6.3	4.8	−0.2	0.3
5.1TAG16	29	36	119				10	35–41			141					−0.2	
5.1TAG15	32	35					11	29–59			163					−0.1	
5.1TAG14		25	136	268	11	48	16	16–42	168	0							0.44
5.1TAG13																	
5.1TAG12	34							21–45			172						
5.1TAG11	29	26						32–60			141					0.1	
5.1TAG10	34	36						28–34			172					−0.2	
5.1TAG9			99														
5.1TAG8	32										163						
5.1TAG7																	
5.1TAG6	27	20	49	92	9	35	9	22–27	145	7	131	0.7	3.4	1.8	2.3	0.4	0,45
5.1TAG5	41	30	138	250	4	34	15	33–36	172	3	228	1.1	6.1	5.0	4.5	0.4	0.1
5.1TAG4	41	22	121								201					0.9	
5.1TAG3	38	32									187					0.2	
5.1TAG2	24										115						
5.1TAG1	30	45	80	160	4	47		58–33	167	21	152	1.0	6.0	3.8	3.6	−0.3	0.09
4.3TAG13	31	36									159						
4.3TAG12	15		95								67						
4.3TAG8	30	22	86	176	5	25		14–24	166	1	152	1.1	5.8	4.4	4.0	−0.3	0.2
4.3TAG7	31	20	107	220					176		159	1.3	7.1	6.1	4.9	0.5	
4.3TAG6	45	24	115	230	0	26		6–18	180	0	217	1	5.1	4.5	4.3	0.7	0
4.3TAG1	46	27	128	249	11	46		6–11	160	−9	236	1	6.5	4.7	4.9	0.6	0.4
4.2TAG1	54	39	122	237	11	60	17	15–23	159	−5	255	0.9	4.4	4.0	4.2	0.4	0.3

Abbreviations: **l**, footprint length; **a**, footprint width; **P**, pace length; **z**, stride length; **Ar**, trackweay deviation; **Lr,** trackway width; $\mathbf{t_e}$, projection of digit **III** (extension of middle digit; **IˆIIˆIII**, Interdigital angles; Ap, pace angle; **O**, footprint orientation; **h**, acetabular hignt; **z/h**, relative stride; **z/l**, stride/footprint length or Steimberg ratio); $\mathbf{v_1}$, speed (Alexander, 1976; Thulborn, 1990); $\mathbf{v_2}$, speed (Demathieu, 1986); **(l-a)/a**, relative footprint length; **Ar/a**, relative trackway deviation.

i) Synsedimentary stage prior to sedimentation after the formation of the footprint. The shape of the footprints depends on the properties of the rocks (composition and grain size, thickness of the strata and layers, sedimentary structures, compaction and degree of water content) of each site at the time of the footprint impression. The structures are different if the study surface (laminites, levels or strata), with footprints, is the tracking surface or some older surface. If they are real undeformed footprints, their depth varies according to the nature of the substrate, and therefore their shape. The difficulty in separating real traces from some undertracks is also known. The most apparent deformation structures of real footprints are either: a) the narrowing of the digits due to collapse - sometimes with the total closure of gaps and with exit structures in front of the foot that has completely penetrated the ground (Fig. 8); b) the collapse of mud displaced by the movement of the foot as extrusion rims and interdigital accumulations of mud (Fig. 9) or; c) the collapse of the digits (Fig. 9) produced by the mud displaced by a neighboring footprint. Among the cases described there are footprints deformed by interference with others, and some induced by landslides on the tracking surface after the footprint impression, as in the 7.3TAG site (Fig. 4).

The shaft of the footprints may be totally or partially filled by sediments from the same broken levels deformed by the foot (Fig. 10). It is defined as a subtrack. The subtrack (*sensu* García Ramos et al., 2002) is a structure formed by fragments of rock from the tracking surface and lower levels intruded by the foot in the hollow of the footprint [cf. Requeta et al., 2006–2007]).

Sometimes the broken sediments only occupy a narrow band at the bottom of the digit traces, in which case they are called base breccia (Boutakiout et al., 2006). In the hollow of the actual footprint, there are also fillings due to mud flows or thixotropic mud flow (Fig. 11) subsequent or simultaneous (Phase K) to the exit of the foot. Sometimes, although the filling material is sediments after the passage of the dinosaurs, the mimicry between the lower material (surface with direct structures) and the upper material (filling) is total.

ii) Sedimentary stage subsequent to the formation of the footprint, but from the same sedimentary cycle (Figs. 12 and 13), in which the shafts are filled (natural casts) by sediments from later sedimentary levels (as in 4.2TAG). Sometimes the natural casts are partially eroded, in which case direct structures such as the dragging grooves of the claws can be seen. Structures of this stage are also the deformation produced by the movement of the sediments that have not yet been compacted; the traces are compressed parallel to the direction of movement, so that they become narrower or shorter depending on their orientation (7.3TAG).

iii) Current stage where recent weathering and erosion lead to the conservation status and shape of the footprints. Two zones are usually distinguished in the sites:
    iiia) The upper part of the 7.10TAG and 4.2TAG sites (Fig. 2) are an example of a very resistant ferruginized level. The brown to black rock surface is covered by a very compact and armored ferruginous crust, smooth and so perfect that the footprints look like true footprints (Fig. 14B).
    iiib) The topographically lowest part is generally light yellow, green and/or grey. In this part, erosion can be seen in the footprints with peeling and loss of fragments (Fig. 14A).

Paradoxically, the upper part is so hardened that it protects the rock and does not release fragments capable of being eroded. We assume the highest outcropping has been more exposed to the weather and for longer than the lowest. In some footprints partially filled with sediments, ferruginization is the reason that it is not possible to distinguish between the nature of the trodden and the filling material.

Undoubtedly, many footprints described in this work are real footprints because they are associated with direct structures (for example, footprints with thixotropic mud fill) or those that preserve claw traces or digital pad traces. But of all of them we have only considered stamps the ichnites from the 7.6TAG site (Fig. 15), which are shallow and maintain the structure of the digital pads with their well-defined separations and with static traces of the claws.

4.2. Ichnotaxonomy

In previous ichnological works on Imilchil footprints (cf. Klein et al., 2022) several ichnotypes have been distinguished. Some of the footprints that we have analyzed in our work have been assigned to them. The assignment is made in an open nomenclature since the variability of the characters of most footprints that we describe is great. In each case, we justify the characters that we use for such an association, considering the reliability of the assignment in each ichnotype.

4.2.1. ***Ichnogenus*** *Changpeipus* ***Young (1960)***

5.1TAG10, 5.1TAG12 (Figs. 6 and 16). The length of the two footprints is 34 cm. They are tridactyl, mesaxonic with strong digits that have lateral constrictions typical of the limits of digital pads; acuminate digits and an asymmetrical shape of the lateral digit position in which the proximal notch of digit **II** is also very evident. The angular asymmetry (**IIˆIII** [24°]<**IIIˆIV** [40°]) is also patent.

4.2.2. ***Ichnogenus*** *Megalosauripus* ***Lessertisseur (1955) (sensu*** *Lockley et al., 1998****)***

The definitions of this ichnotaxon can be applied to several of the footprints from the Imilchil sites.

For example, in the trackway of the 4.2TAG site (Figs. 3, 6 and 14) the footprints have a typical diagnosis of the ichogenus of *Megalosauripus*: giant footprints **l** > 50 cm (mean length 54 cm and mean width 39 cm) and narrow ([**l-a**]/**a** = 0.4, or what is equivalent **l**/**a** = 1.4) with robust and separated digit traces with acuminate termination, sometimes with sharp claw traces. The proximal pad of the fourth digit is usually on the heel. Digit divarication indicates that digit **II** diverges less from **III** than digit **IV** (**IIˆIII** [15°] < **IIIˆIV** [23°]), The height of the acetabulum is 2.5 m and the Sternberg ratio low (**z**/**l** = 4) The trackway is very narrow (**Ar**/**a** = 0.4) although the pace angulation is not very open (**Ap** = 158°), the footprint orientation is negative and the trajectory is sigmoid, with an irregular long-short pace sequence. The displacement is at a moderate speed (**v** = 4.1 Km/h). Variable characters among these footprints are the mexasony, the shape of the heel with: a pronounced metatarsal trace, a bilobed trace or a notch (or not) in the proximal part of digit **II**. If these variable characters were in footprints from different trackways, they could lead us to assign the footprints to several ichnotypes.

Also very apparent is the similarity between the footprints from the Taghighacht 1 site cited by Klein et al. (2022, Fig. 13) and many of the 4.3TAG footprints (Figs. 3, 6 and 13). This site consists of isolated natural casts on a surface with ripples. Of these, the footprints of trackways 4.3TAG1, 4.3TAG6 and 4.3TAG7 are especially similar to those of Taghighacht 1. The footprints are also large (**l** = 46, 45 and 31 cm; **a** = 27, 24, 20 cm) and narrow ([**l-a**]/**a** = 0.6, 0.7.0.5). The digits are robust and separated. In 4.3TAG1 the heel is located in the proximal pad **IV** (in 4.3TAG6 and 4TAG7 such position is not clear). In the digits where the tip is preserved, their termination is acuminate. The digit divarication is low, (**IIˆIII** [6°]<**IIIˆIV** [15°]). The value of the Sternberg ratio is highly variable (**z**/**l** from 5.1 to 7.1). The trackways are very narrow (**Ar**/**a** between 0 and 0.4) which is consistent with the pace angulation values (**Ap**, 160, 180 and 176°) and with relatively long strides (**z** ≈ 2 P).

In the western part of 7.3 TAG, there are two deformed types of large footprints whose shape depends on their orientation: the first, N/NW-S/SE in orientation, are usually large with wide and separated digit traces (Fig. 17A), some of which have an acuminate termination; the second,

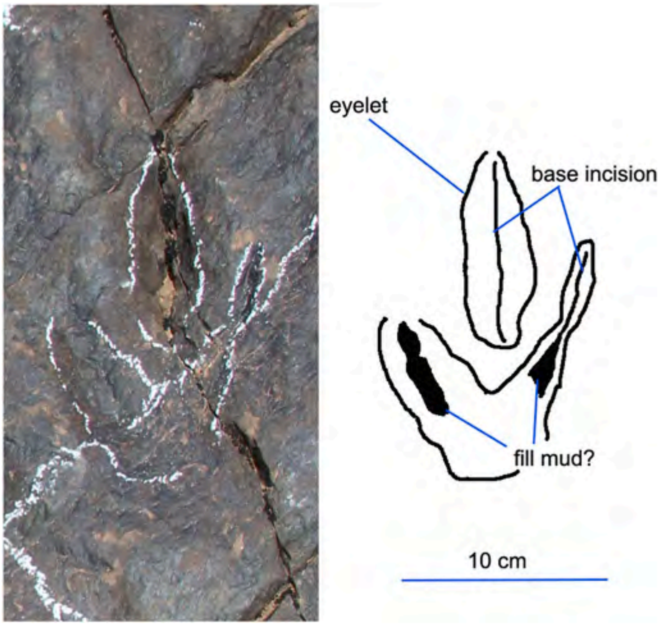

Fig. 8. 7.7TAG11.2. Mud structures in the footprint of the foot immersion (slash-like incision, closure of the proximal part of digit III mark) and exit (eyelet). Sediment filling after the exit of the foot on the proximal part of the II and IV digit marks. Apparently the composition of the tracking level and filling is similar.

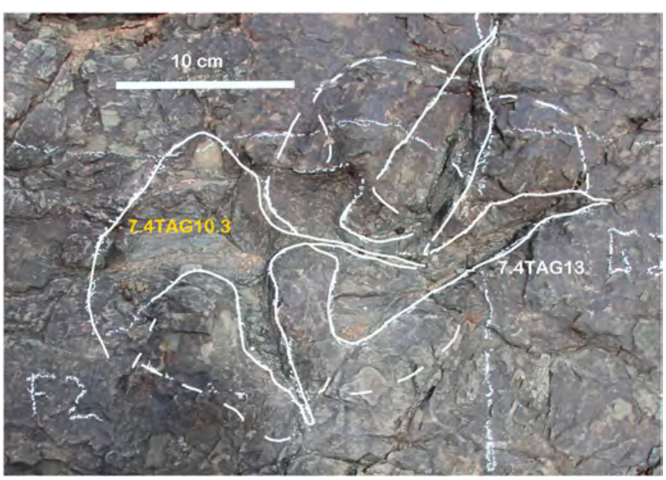

Fig. 9. Collapse structures (base striae or base incisions) at the bottom of the digit marks. Mud extrusion at the front of the footprint, between the digits, expelled by the foot and pushed forward (during T phase). Collapse of digit IV of 7.4TAG13 due to gravitational fall of the mud. Closure of the walls of digit IV of 7.4TAG10.3 by mud displaced by 7.4TAT13.

NE-SW oriented, have narrow and long digit traces (Fig. 17B). In this site there are mud slide structures. The former can be associated with *Megalosauripus* and it is possible that part of the latter are of this same ichnogenus but deformed.

At 7.4TAG west (Figs. 4 and 6), most of the tracks are tridactyl, mesaxonic, some with pad traces, variable interdigital angles, and have mud between the digits (Fig. 10) - probably accumulated in the entry movement of the foot, pushing forward. Similar examples can be seen both in ornithopod footprints (El Contadero site, Pérez-Lorente et al., 2000), and in theropod footprints (Las Mortajeras site [Casanovas et al., 1993]), or in footprints that completely introduce the foot into mud (theropod footprints at the Santisol site, Pérez-Lorente, 2003, 2015). We assign them to *Megalosauripus* because of their morphology and their

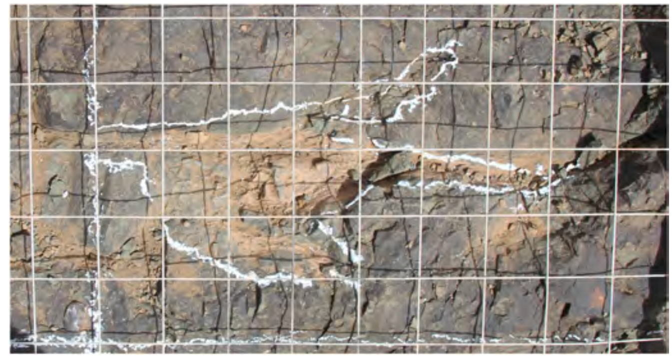

Fig. 10. Subtrack 7.4TAG3.2 with the shaft partially filled with material deformed during the treading. Mesh, 5 × 5 cm.

size, generally more than 28 cm in length (Lockley et al., [1998] defined *Megalosauripus* as a tridactyl footprint, of medium to large size). The same authors also specify that their occurrence is limited to the Middle-Upper Jurassic, and that they are the major theropod footprints of the Jurassic.

The footprints of the 7.5TAG site (Figs. 4 and 6) that form part of a trackway and two isolated footprints can be included in this ichnotaxon. The footprints of the 7.5TAG1 trackway are between 37 and 44 cm long, are longer than wide (**a** between 27 and 34 cm), have strong, separated acuminate digits. The footprints show angular (**IIˆIII** [12°] < **IIIˆIV** [24°]) and positional asymmetry with digit **IV** beginning at the heel and toe **II** more advanced and leaving a proximal notch.

In 7.8TAG site (Fig. 5) there are two types of footprints that are separated by their size; 24 are over 38 cm long (Fig. 6) while the others (4 unidentified footprints) are less than 19 cm. In some large footprints, despite the fact that erosion has lifted fragments of the layer that have marred the footprints, traces of digital pads and sharp claws are recognizable. The footprints are large (mean length is 44 cm) and narrow ([**l-a**]/**a** = 0.6); they are tridactyl mesaxonic; the heel shape is variable even between footprints of the same trackway (7.8TAG7), although it is usually recognized that the heel is formed by the proximal pad of digit **IV** and also have the notch of the outline associated with the proximal part of digit **II**. The value of the digit divarication is highly variable **IIˆIII** (between 2 and 25°) but always less than the value of **IIIˆIV** (between 13 and 35°).

7.10TAG3 are footprints that are long (**l** = 37 cm) and narrow ([**l-a**]/**a** = 0.4); with wide digit traces, some with acuminate termination, with clear angular asymmetry (**IIˆIII** < **IIIˆIV** [13° < 27°]). These are no collapse (Figs. 5 and 6) or deformation structures. They have relatively large pace (**P** = 102 cm) and stride (**z** = 196 cm), and pace angulation (**Ap** = 130°) and the Sternberg relation (**z/l** = 5.7) is relatively small.

Míguez Minguez Ceniceros et al. (2022) mentioned the possibility that the two colossal footprints from Imilchil (4.5TAG1 and 7.10TAG19) could be assigned to *Megalosauripus*.

4.2.3. *Ichnogenus* Trisauropodiscus *Ellenberger (1970)*

5.1 TAG (Fig. 3) is a site with 58 tridactyl footprints that generally have long, very narrow digit traces (Fig. 18), sometimes somewhat sinuous, and separated. The exceptions are footprints 5.1TAG10, 5.1TAG12, with wider and short digits, and trackway 5.1TAG22 in which the footprints also have a metatarsal trace (Fig. 6). The digit traces are usually crossed along by a base striae and the walls are formed by folded laminites, dragged by the digits (Boutakiout et al., 2006; Hadri and Pérez-Lorente, 2012; Gatesy and Falkingham, 2020). The heel shape is highly variable as well as the value of the angle of digital divarication **IIˆIV** (between 38° and 91°) that can exceed 90°. The length of the footprints varies between 41 and 24 cm, and it is noteworthy that in many of them, the length of digit trace **III** from the hypex is greater than 2/3 of the total length of the footprint.

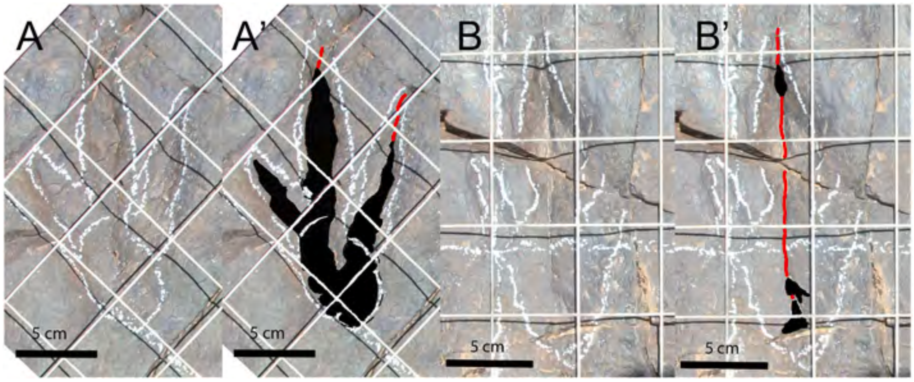

Fig. 11. Partial filling of traces of the 7.7TAG site by mud flow. A//A′ 7.7TAG5.10; B//B′, 7.7TAG5.6, with dragging groove of the claw of digit III, distal part of digit IV partially filled. Outline (white); filling (black); base incision and drag striae (red). The striae and incisions predate the mud filling.

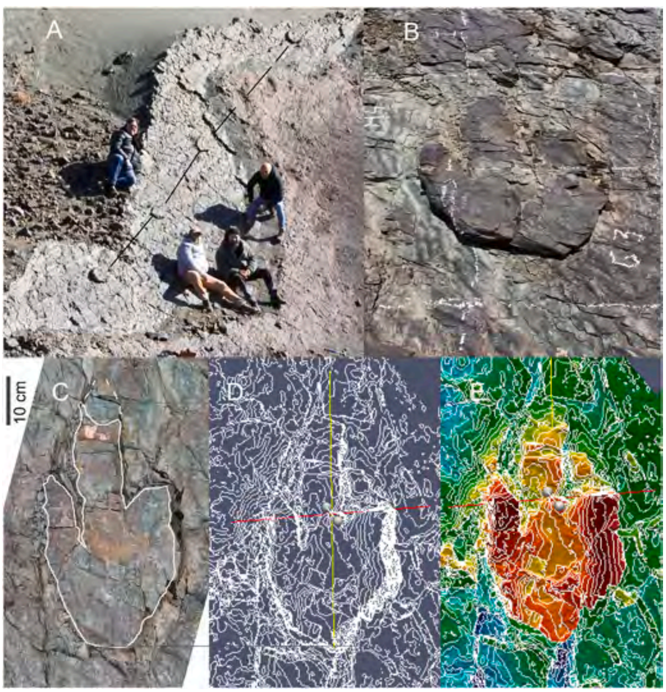

Fig. 12. A, eastern part of 4.3TAG site, natural casts of 4.3TAG1 trackway (4.3TAG1.4, 4.3TAG1.5, 4.3TAG1.6, and 4.3TAG1.11); B, 4.3TAG1.2 (chalk mesh, 30 × 30 cm); C, D, E, 4.3TAG1.4: C, outline; D, contour lines; E, color elevation.

In 7.3TAG there are several small footprints (7.3TAG14//7.3TAG19) less than 19 cm, longer (**l** = 15?//19 cm) than wide (**a** = 11?//15 cm) and narrow ([**l-a**]/**a** = ?//0.1), probably with collapse structures that narrow the digit trace. One of these footprints (7.3TAG19.2) shows a *Trisauropodiscus*-like shape: slender digit traces; relatively high divarication **II^IV** = 60°; digit **III** much larger than the lateral ones, and an elongated trace at the position of the hallux. It should be noted that it has a base breccia and deformed laminites.

Klein et al. (2022) note that the footprints assigned to *Trisauropodiscus* in Imilchil may be deformed footprints in the sense indicated by Gatesy and Falkingham (2020).

4.2.4. *Ichnotypus Grallatoridae indet*

All the footprints of the 7.6TAG site (except 7.6TAG5) are of the same ichnotype: small footprints (**l** between 12 and 18? cm) longest than wide (**a** between 10 and 11 cm) and narrow ([**l-a**]/**a**, between 0.4 and 0.8); all tridactyl except 7.6TAG6 in which there is a trace that may be

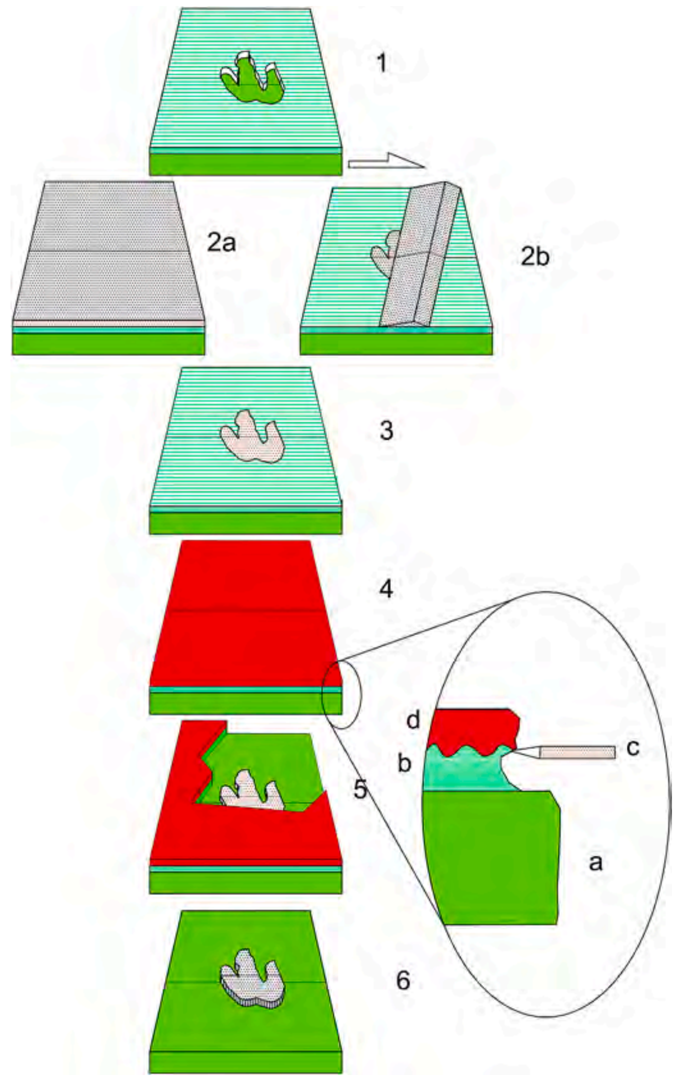

Fig. 13. Filling mechanism and position of the 4.3TAG natural cast in a stratigraphic scheme. On a surface with ripples, footprints (1) that are later filled by a layer (2a) or by the filling of hollows produced by transported sediments (2 b, 3); In 2a, the water flow erodes the sediments that are not in the hollows (3); subsequent sedimentation fossilizes the natural casts (4) which now partially (5) or totally (6) can be seen.

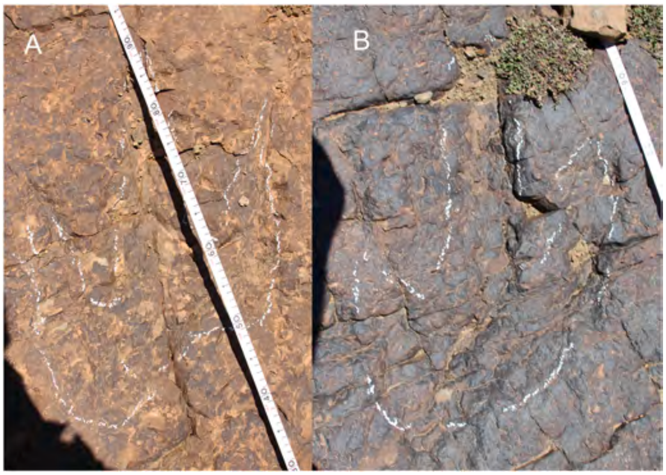

Fig. 14. A,.2TAG1.1 footprint in the topographically lowest part of the study surface with scaling and yellowish-brown and reddish-brown colors; B, footprint 4.2TAG1.11, in the topographically highest part of the site with resistant black crust (no scaling or signs of erosion).

Fig. 15. 7.6 TAG site. Shallow footprints with pad marks.

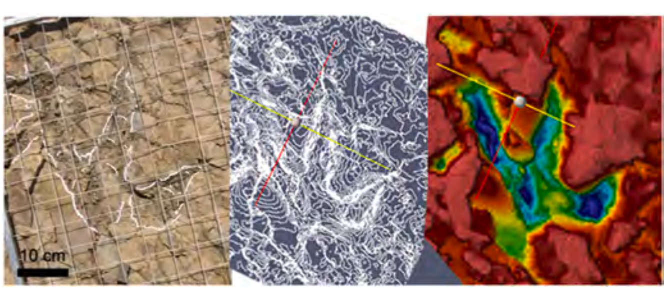

Fig. 16. *Changpeipus*: A, partial overprinting of 5.1TAG12 with 5.1TAG13 (only part of which is visible); A, outline; B, contour lines and pad marks; C, color elevation.

from the hallux. The digit traces are acuminate at times with sharp claw traces, and have well-defined pads, with a clear metatarsophalangeal pad of digit **IV**; digit **III** is usually relatively well projected forward. The shape of the heel is varied but consistent with this type of footprint (Figs. 4, 6 and 15) and can be protruding (7.6TAG7, 7.6TAG1.3), bilobed (7.6TAG3, 7.6TAG1.1) or with non-characterizable lobes (7.6TAG2). The value of the interdigital angles is variable, although in all the footprints it is true that **IIˆIII** < **IIIˆIV**, the mean value being 13 < 32° and the divarication value **IIˆIV** = 50°. The only trackway of the site (7.6TAG1) is composed of three footprints and is very narrow (**Ar/a** = 0.3), according to the value of **z** (72 cm) = 2**P** (36 cm) and with a very open pace angulation (**Ap** = 170°). The height of the acetabulum is about 170 cm, the speed of movement is slow (3.8 km/h) and the Sternberg ratio is high (**z/l** = 8).

4.2.5. *Unidentified footprints*

In almost all the sites there are footprints, generally isolated, which are unclassifiable due to their degree of deformation or preservation. We cite below the cases in which the limit line allows us to deduce the characteristics that define them.

The footprints of the 7.1TAG site are very deformed footprints due to the fact that the foot penetrates into soft soil, leaving base striae, scars or slash-like incisions (Gatesy, 2003). Subsequent to the formation of the incisions, the walls of the footprints fall, deforming by collapse. In general, the current digit traces are long and thin (Figs. 1, 4 and 69A). The same thing happens to the tridactyl footprints of 7.2TAG in which, for example: 7.2TAG5.2 has a very long digit **III**, base striae with deformed laminites and wall collapse (Figs. 4 and 19B).

The tridactyl footprints from the 7.4TAG east site (Figs. 4 and 19C), have narrow digit marks in which the folded laminites are found (in the same way as those mentioned by Hadri and Pérez-Lorente (2012) and Gatesy and Falkingham (2020)), and angle **IIˆIV** is very open, as in bird footprints. In the 7.4TAGn site, the tridactyl footprints (pair 7.4TAG5) have clear outlines, are small, with a rounded heel and a divarication of 58°; part of the filling of the tracks is preserved (Fig. 4). We do not know if the filling is deformed (subtracks) or not (natural casts). Due to their size, they could be associated with *Dineichnus*, but the two footprints of the 7.4TAG5 pair are not symmetrical.

In 7.7TAG the color of the study surface is very dark brown to black due to the metal oxides it contains. The footprints are small (**l** = 16 cm, values between 12 and 20 cm), narrow ([**l-a**]/**a** = 0.4) and almost all included in trackways. Relatively shorter footprints with short, wide digit traces are positioned parallel to the NS direction. Many footprints have base striae at the bottom of the digit traces, partially hidden by the filling of the same color and apparently the same texture as that of the trodden sediment (Fig. 11). This indicates that it is a tracking surface with striations produced by the claws, filled with later fallen mud. It is possible that, given the conditions of the sediment (deformed when it was still soft) there was thixotropic flow towards the interior of the footprints. The surface of the stratigraphic bed is deformed, probably by synsedimentary slippage, and we do not know the true dimensions and shape of either the footprints or their structures (digit, pad or claw traces) or the interdigital angles.

The footprints of the 7.10TAGF1, 7.10TAG2, 7.10TAG5 trackways and the tridactyl isolated footprints from the 7.10TAG site are small (**l** varies between 22 and 14 cm) narrow ([**l-a**]/**a** between 0 and 1). All of them are deformed with collapse structures (Fig. 20), accompanied or not by base striae, which narrow or even close the digit mark, or by structures associated with foot penetration in very soft mud. In general, they tend to have a very long digit mark **III** compared to those of digits **II** and **IV**, which are very short and very open, similar to those produced by the foot advancing when sliding inside the mud. The trackways are very narrow (**Ar/a**<0.5).

The outline of the footprints in the 7.10TAG7 trackway, only allows us to know that the autopodia were tridactyls, or that they had three front digits (Fig. 5). These footprints are oval shafts in which the anteroposterior axis is the largest. In 7.10TAG7.4 the shape of the footprint in which the digits are distinguished and the triangular shape of the contour of the footprint can be seen. These footprints may be traces or, as has already been interpreted (Masrour et al., 2021), morphologies due to the thixotropic flow of mud from the walls once the foot has emerged from the mud.

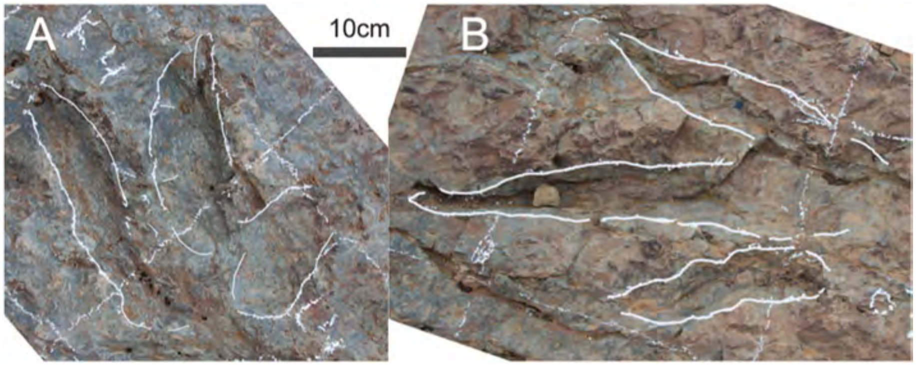

Fig. 17. *Megalosauripus*: A, 7.3TAG16.2 footprint axis positioned parallel to direction of shortening; B, 7.3TAG22.1 with the footprint axis placed perpendicular to the shortening.

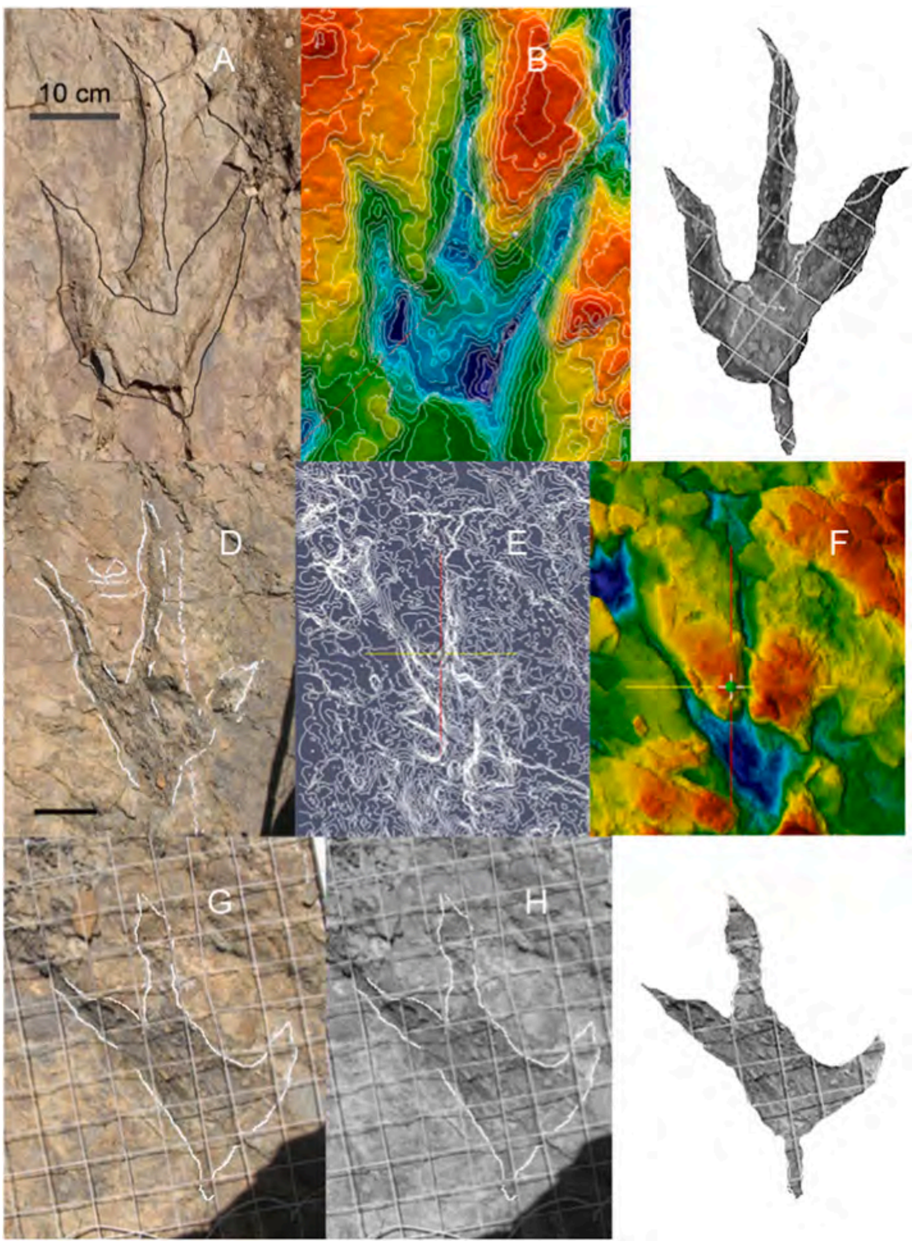

Fig. 18. *Trisauropodiscus*. 5.1TAG24.1 footprint (A, outline; B, contourlines and color elevation; C, grey footprint image). 5.1TAG25 trackway: 5.1TAG25.3 (D, outline; E, contour lines; F, color elevation); 5.1TAG25.2 (G, outline; H, grey image; I, grey footprint image). You can see: the hallux? mark or, a deformation structure? the variability divarication and measurements of digits; and the morphological variability of the footprints even within the same trackway ones. Deformation structures produced by the passage of the digits through the sedimentary laminites are shown in 5.1TAG24.1 and 5.1TAG25.3.

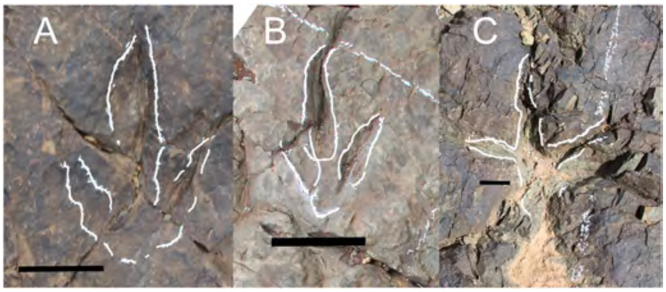

Fig. 19. Mud collapse structures with narrowing of the walls of the digit marks, and with base incisions. A, 7.1TAG1.3; B, 7.2TAG5.2; C, 7.4TAG2.3. Scales: in A and C, 5 cm; in B, 10 cm.

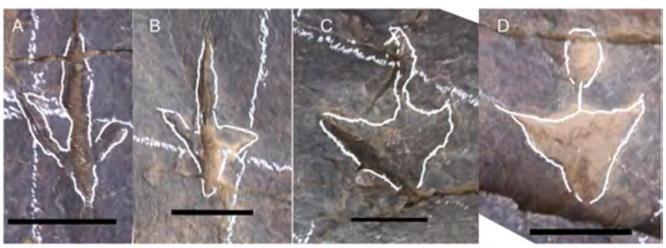

Fig. 20. Structures in small tridactyl tracks from the 7.10 TAG site: A, 7.10TAG2.1, thinned digit marks produced by wall collapse, and visible base incisions on lateral digit marks; B, 7.10TAG2.4, base striae on all three digits, trace of digit III is abnormally elongated; C, 7.10TAG1.5,slash-like incisions on all three digit traces, advanced traces of the lateral digits, and almost complete collapse of the central digit; D, 7.10TAG1.7, slash like incisions of the II, IV digit traces, exit eyelet of the foot, advanced traces of the lateral digits and narrow cleft structure or total collapse of the metatarsal passing. Scale in all photographs, 10 cm.

4.3. *Morphometry*

4.3.1. *Size of theropod footprints from imilchil*

4.3.1.1. Length of imilchil footprints. The length of the Imilchil footprints we have worked with ranges from (Table 2) **l** = 8 cm (7.6TAG1.2, the smallest) to **l** = 76 cm (4.5TAG1, the largest). The value of the smallest (Table 2) is not considered in any of the analyses because that footprint is in a trackway (7.6TAG1) whose average length is **l** = 10 cm (Table 3). The histograms have been constructed with the number of trackmakers and not with the number of footprints. There are incomplete footprints, sometimes all from the same trackway that cannot be measured. For this reason, in the Imilchil histogram there are 101 data of the 138 deduced trackmakers. These data correspond to: 9 dinosaurs whose footprints are very small (less than 15 cm); 31 dinosaurs with small footprints (15–24 cm); 55 with large footprints (25–49 cm); 4 with giant footprints (50–69 cm); and 2 with colossal footprints (greater than 70 cm).

Fig. 21 shows the histograms of Imilchil, Iouaridène and La Rioja (authors' data) that indicate a group of very small-small footprints in Imilchil (**l** = 14–18 cm); very small in La Rioja (**l** = 12–14 cm) and not defined in Iouaridène). This separation is similar to what some authors have pointed out (Thulborn, [1990]; Pérez-Lorente and Romero-Molina [2001]). In small sites, or located in selective habitats (Thulborn, 1990; Lockley et al., 1983), they have served to interpret population groups, with hypotheses that consider individuals of the same species and different sizes or individuals of several species (see also Shell and Boss, 2013). In histograms of large areas (Fig. 21) the associations should be of individuals of more than one ichnogenus and in different habitats (lacustrine, marshy, fluvial, …) even if they are from the same environment.

The diagram (Fig. 21) shows the number of individuals depending on the length of their footprints at the Imilchil (138), La Rioja (217) and Iouaridène (94 individuals) sites. It is not an up-to-date diagram because both in La Rioja and in Iouaridéne there is data subsequent to the preparation of the histograms (e.g.: Boutakiout et al., 2009; Pérez-Lorente, 2003) of some new sites, described or not.

By size, two separate sectors are observed (Fig. 21). We have found this trend in La Rioja where there is a grouping in the smallest footprints (15 cm in length), another centered in the vicinity of 32–34 cm in length, and, separated from the set, some residual giant and colossal footprints. If the projection of the footprint data is made based on the length and width of the footprints (Pérez-Lorente and Romero-Molina, 2001), the diagram shows the three groups in which the footprints are separated (Fig. 21).

However, in the three histograms there is the same trend: a group of very small-small footprints separated (Table 4) by a minimum of another group of large-colossal footprints. To the right of the second maximum of the large footprints (**l** > 38 cm), the size declines to leave some giant-sized footprints and some evidence of colossal footprints. This separation in the diagram of a group of minor trackmakers was already highlighted in their diagrams by Pérez-Lorente and Romero-Molina (2001).

This distribution can be inferred by separately examining the footprint size histograms with the footprints studied from the three environments (Fig. 21), and by superimposing all the data. As the separation between the minor trackmakers and the rest is apparent (around **l** = 20 cm), it can be proposed that such distribution of small and large individuals is due to the fact that a sector of the medium-sized theropod trackmakers is in the minority or is absent, at least in the computation of these deposits. The lack of footprints in the small-large sector indicates that there were no dinosaurs with that foot size. The explanation may be similar to that of the change in the ontogenetic niche (ONS model) of dinosaurs of a certain size (Schroeder et al., 2021; Lockley and Xing, 2021), but also to the coexistence of individuals that are small in adulthood and the entry of dinosaurs that, starting at a certain size, are incorporated into the ecological niche of adult dinosaurs (small and large).

The separation by the footprint length of the group of minor dinosaurs is also evident in other diagrams (Pérez-Lorente and Romero-Molina, 2001). The gap in footprints between the very small-small group and the rest speaks of a lack of population that can be attributed to the coexistence of two different types (adults with small-very small footprints and dinosaurs that have larger footprints as adults). It is clear that no intermediate print has been impressed. This can be attributed to a change in the ontogenetic niche of dinosaurs in general, or to a population of small-sized dinosaurs and the entrance of larger-sized dinosaurs that were not originally there.

4.3.1.2. Footprint length and footprint width. Imilchil tridactyl footprints are generally longer than they are wide (Figs. 22 and 23). The variation of the length of the footprint as a function of its width (0 < [**l**-**a**]/**a** < 1) is within the range of narrow footprints (value of **l** between **a** and 2**a**). The maximum of the histogram (Fig. 22) is reached when the ratio of the length of the footprint is one and a half times its width ([**l**-**a**]/**a** = 0.5).

The projection of the length of the footprint as a function of the width (Fig. 23) is mostly below the line **l** = **a**, that is, they generally meet the theropod condition. We do not have the elaborated data for Iouaridène, but we do have those for La Rioja, and the fit between both sets of footprints can be seen (Fig. 23). This diagram is even more explicit in the separation of the group of very small-small footprints. Imilchil footprints tend to be longer relative to their width than those from La Rioja.

4.3.1.3. Other measurable characters. Digit divarication between the axes of the digit prints is independent of their length or the distance between the proximal part of the digits and the axis of the footprint. The value of divarication is highly variable in the examined trackways, and

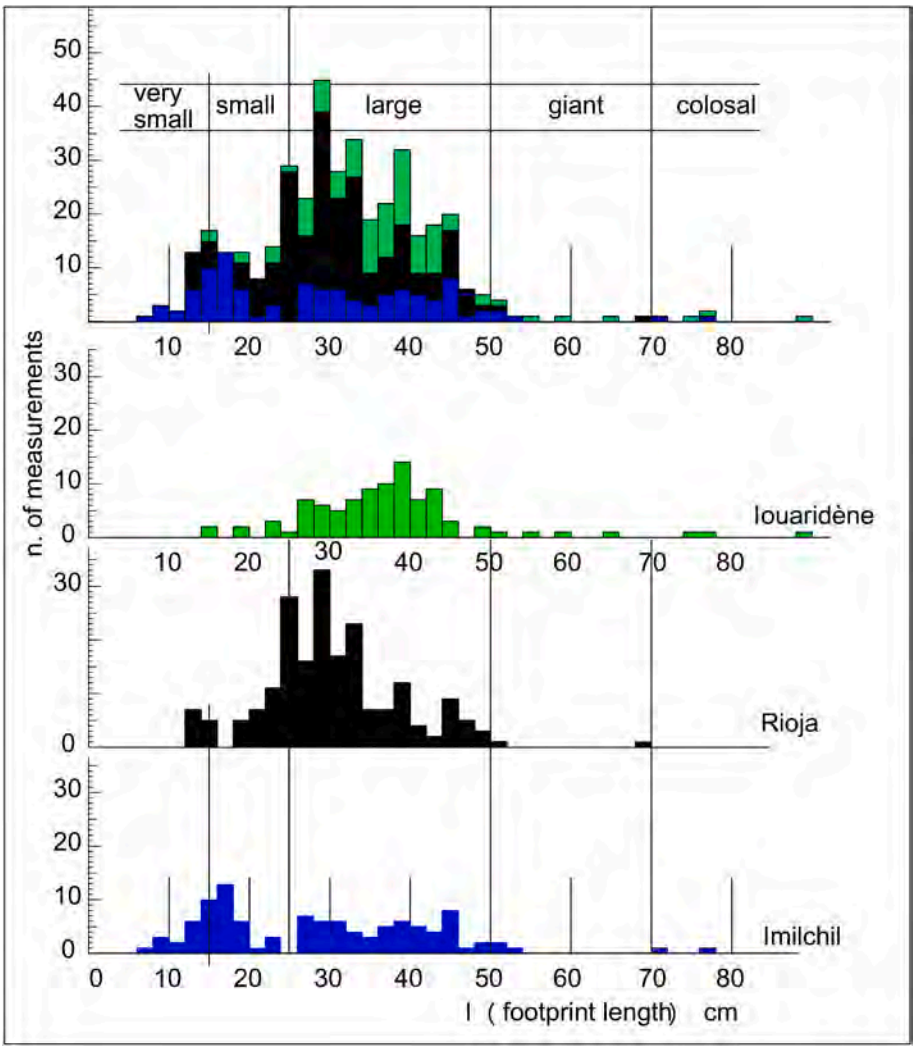

Fig. 21. Histogram with the projection of the length of the theropod footprints - one for each trackmaker - of three macrosites: Imillchil, Iouaridène and La Rioja. It is observed that a group of footprints of **l** < 17 cm can be separated (cf. Minguez Ceniceros et al., 2022).

Table 4
Maximuns and minimuns in the footprint length data.

Sites	Maximum	minimum	maximum	minimum	maximum	zero footprints		greater footprint
Imilchil	14–18	20–26	26–28	34–36	44	54		76
La Rioja	12–14	16–18	?	34–38	44–46	52		70
Iouaridene	?	?	26–28	30–32	38–40	52		90
very small	15	small	25	large	50	giant	70	colossal

Measurements in cm.

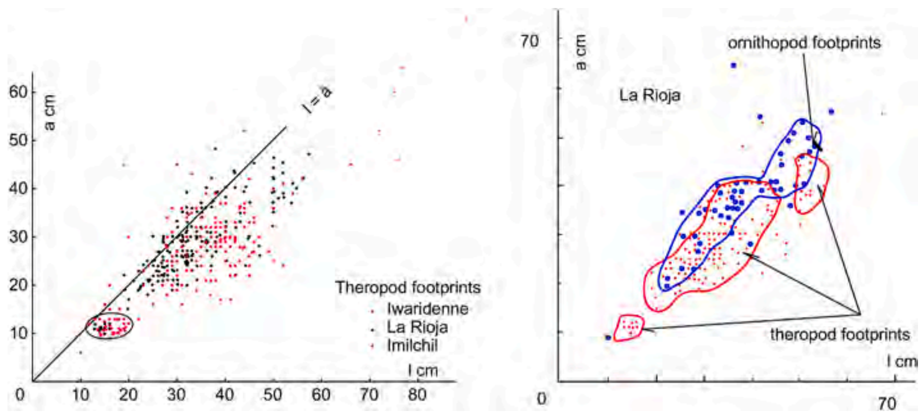

Fig. 22. Representation of the theropod footprints of Imilchil according to their width. Most of them are narrow ([**l-a**]/**a** > between 0 and 1), **A**, projection of the mean values of (**l**–**a**)/**a** of each trackway and the values of all isolated traces. **B**, it has been done with the average values of (**l**–**a**)/**a** of the footprints of each trackway and those of the isolated footprints.

even between the footprints of the same trackway. If the divergence is measured taking into account the axes of the digits, it is observed (Tables 2 and 3) that the difference between the value of the interdigital angles (**IIˆIII** < **IIIˆIV**) is usually maintained. It is possible that the divergence varies greatly depending on the depth of the track, the deeper it is, the more open it is (Thulborn, 1990).

4.3.2. Metric relationships between footprints and trackways

4.3.2.1. Relationship between footprint length and stride. The relationship between the length of the footprint and the stride is linear (Pérez-Lorente, 1996). This indicates that there is a relationship

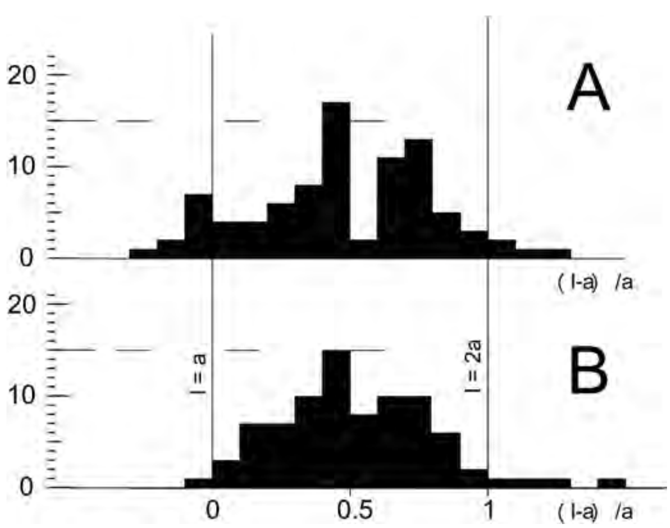

Fig. 23. Representation of the Imilchil footprints according to the **l**/**a** ratio. This diagram shows more clearly the separation of the group of small dinosaur footprints: the values in Imilchil and La Rioja overlap. Each point is one trackway. The footprints of Imilchil are proportionally longer than those of La Rioja.

between both theoretically independent variables. Or put another way, the variation of the stride in relation to the length of the footprint (Fig. 24B) is limited: encompassed between two straight lines ($\mathbf{l} = \mathbf{z}\ \mathrm{tg}\alpha + 5.7$ where $10°37' > \alpha > 3°17'$).

When comparing the data from Imilchil with those from La Rioja, it is confirmed that they are congruent in this projection. In diagrams (Fig. 24A and 24C), the straight lines represent the **z**/**l** ratio defined by Sternberg (1926) and used by Casanovas et al. (1989) as possible indicators of the slenderness of the locomotor limbs of bipedal dinosaurs.

The speed equations of Alexander (1976) and Demathieu (1986) indicate the little influence of the speed of the dinosaurs studied on the linear relationship between **z** and **l**. Although in the formulas of the previous researchers the speed is a function of **h** and **z**, we know that **h** (Thulborn, 1990) is a function that depends on the product of **l** by a constant. In other words, the variation in speed obtained in the dinosaur trackways in La Rioja and Imilchil do not allow the points of the projection to go outside the interval determined by the straight lines in Fig. 24B.

The small-footed trackmaker group is well separated in Fig. 24A. It is diluted in Fig. 24C due to the stride values between 105 and 140 cm obtained in the Imilchil trackways whose stride length ranges between 13 and 18 cm.

4.3.2.2. Relationship of the footprint length and the speed. Studies on speed variation with respect to other morphometric parameters (**l**, **z**/**l**) published on ornithopod footprints (Casanovas et al., 1995) show that the line that represents such variation in a cursoriality ratio diagram (**z**/**l**) with speed ($\mathbf{v_1}$, $\mathbf{v_2}$) is a sector of parabola. This same curve sector is intuited with theropod footprints (Pérez-Lorente, 1996; Pérez-Lorente and Romero-Molina, 2001).

If the speed data ($\mathbf{v_1}$, Alexander [1976]; $\mathbf{v_2}$, Demathieu [1986]) are projected in relation to the length of the footprint (Fig. 25), the diagram indicates that the maximum of the speed envelope is associated with footprints of about 30 cm in length and that the maximum speed is reached in trackways made by large to very small footprints. The tracks from Imilchil (Fig. 25B) are projected onto the same point cloud (Fig. 25C) as those trackways (theropod and ornithopod) from La Rioja

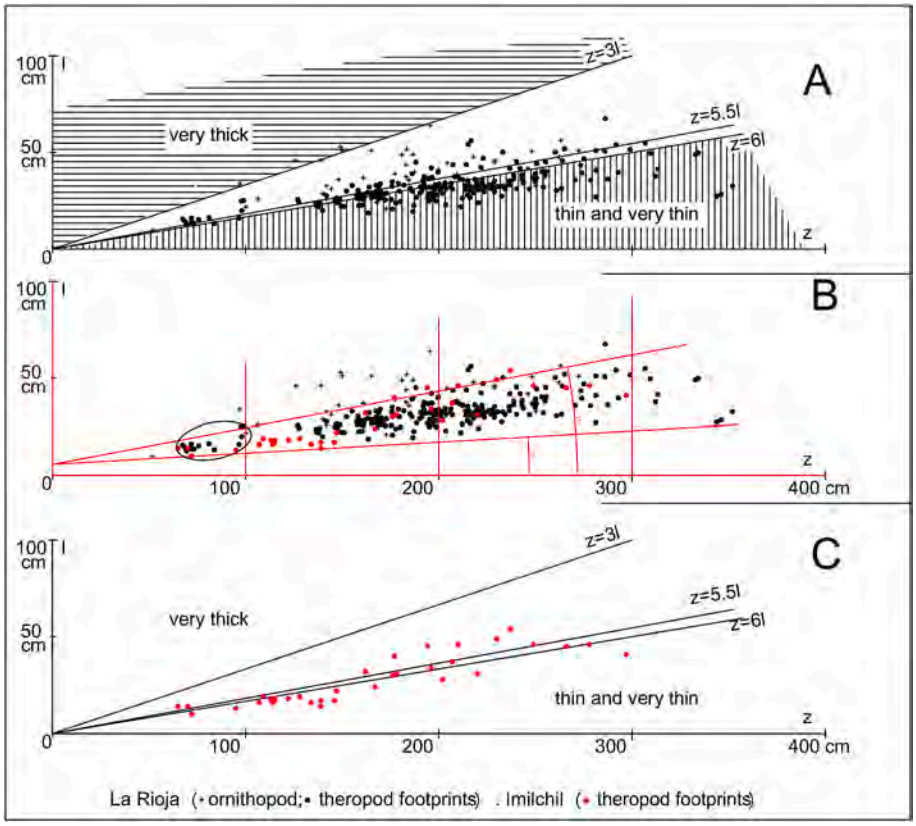

Fig. 24. Projection of the length of the footprints (**l**) in relation to their stride length (**z**): A, projection of the bipedal footprints (theropod and ornithopod) from La Rioja - the diagram shows the straight lines of the Sternberg relation used by Casanovas et al. (1989) to distinguish them by the slenderness of their locomotor limbs; B, projection of the bipedal footprints of La Rioja and Imilchil - two straight lines have been drawn that include the point cloud, and in an ellipse are represented the small footprints separated by Pérez-Lorente (1996); C, projection of the Imilchil theropod footprints.

(Fig. 25A). In the diagram it is observed that for low speed values, the footprint length is of small footprints and giant footprints, while high speed values are associated with large footprints (30–40 cm).

In summary, low speed is associated with giant, small and very small footprints, while high speed is associated with large footprints. Since the data is from the total number of footprints examined, the result should be considered as a general pattern of behavior for all dinosaurs.

As can be seen (Fig. 25) the data from Imilchil are consistent with those found in La Rioja.

4.3.2.3. Relationship of the footprint length and footprint orientation. According to the reference works (Pérez-Lorente, 2001) the orientation has a more negative value (sensu Leonardi, 1987) in the largest footprints. This observation is more evident in ornithopod footprints than in theropod footprints (Pérez-Lorente, 1996; Pérez-Lorente and Romero-Molina, 2001). 79% of the theropod footprints from La Rioja (Fig. 26) have an orientation of 0° or a negative value. The Imilchil data (Fig. 26) fit the same scheme. In the diagram that shows the orientation of the theropod footprints as a function of the length of the footprint, the separation of three groups can be seen. The variation of the orientation for the small-very small footprints is large and mostly positive.

4.3.3. The trackways

4.3.3.1. Direction of dinosaur progression. The orientation of the trackways (straight line joining the center of the first and last footprints) and that of the isolated footprints (footprint axis) have been measured and projected. All footprint-bearing layers have been folded so that the orientation is measured on a horizontal plane. In total, 111 measurements have been reported (Fig. 27) in two graphs: i) a compass rose in which the orientation and direction of movement of the animals can be clearly seen; and ii) two histograms to visualize the maxima found.

Intervals of 10° have been taken to count and group the trackways and isolated footprints according to their orientation and direction of travel. In the histograms of Fig. 27 (with and without the data of isolated footprints) it can be seen that the variation is notable, but that the distribution by maximum and minimum is similar. It is observed that the two predominant orientations are NE and ENE-WSW and the predominant direction of travel is towards the NE and ENE.

In the data published on La Rioja tracksites by Martín Escorza (1988, 2001) and by Moratalla and Hernán (2010) it is argued that the footprints and trackways indicate the sites as "preferred regional routes" possibly related to migration limited by paleogeographical conditions (Martín-Escorza, 1988, 2001), or they are paleogeographical limitations without implying migratory movements (Moratalla and Hernán, 2010). Doublet (2004) argues that in the Enciso Group (the stratigraphic unit with the most footprints studied in La Rioja) the paleogeographic model implies a strip of passage and easy stay for dinosaurs, between the edge of a lake and the area of dense vegetation that flanks it.

Between the two works by Martín-Escorza (1988, 2001) and Moratalla and Hernán (2010) there is a strong difference in orientation and direction of travel: the first author worked with the direction of the footprint axis (with a small sample) and the second with the direction of the trackways (with a larger and more extended sample in the area). According to Moratalla and Hernán (2010) the footprints of the same trackway can vary up to 20° with respect to the direction of travel.

For us it is an unsolved problem because the general orientation also depends on the length of the trackways and the sigmoid sector that we observe in the outcrop. In theory, the most apparent trackways are those that coincide with the direction of the greatest length of the outcrops, with directions parallel to the regional orientations. This is more noticeable in places with abundant small and elongated sites that tend to coincide with the regional direction; hence the importance of the orientation of the isolated footprints.

The orientation of the dinosaur trajectories should depend on environmental and climatic factors and the behavior of the dinosaurs. However, the paleogeographic configuration must be a strong conditioning factor in the determination of favorable passages for most of

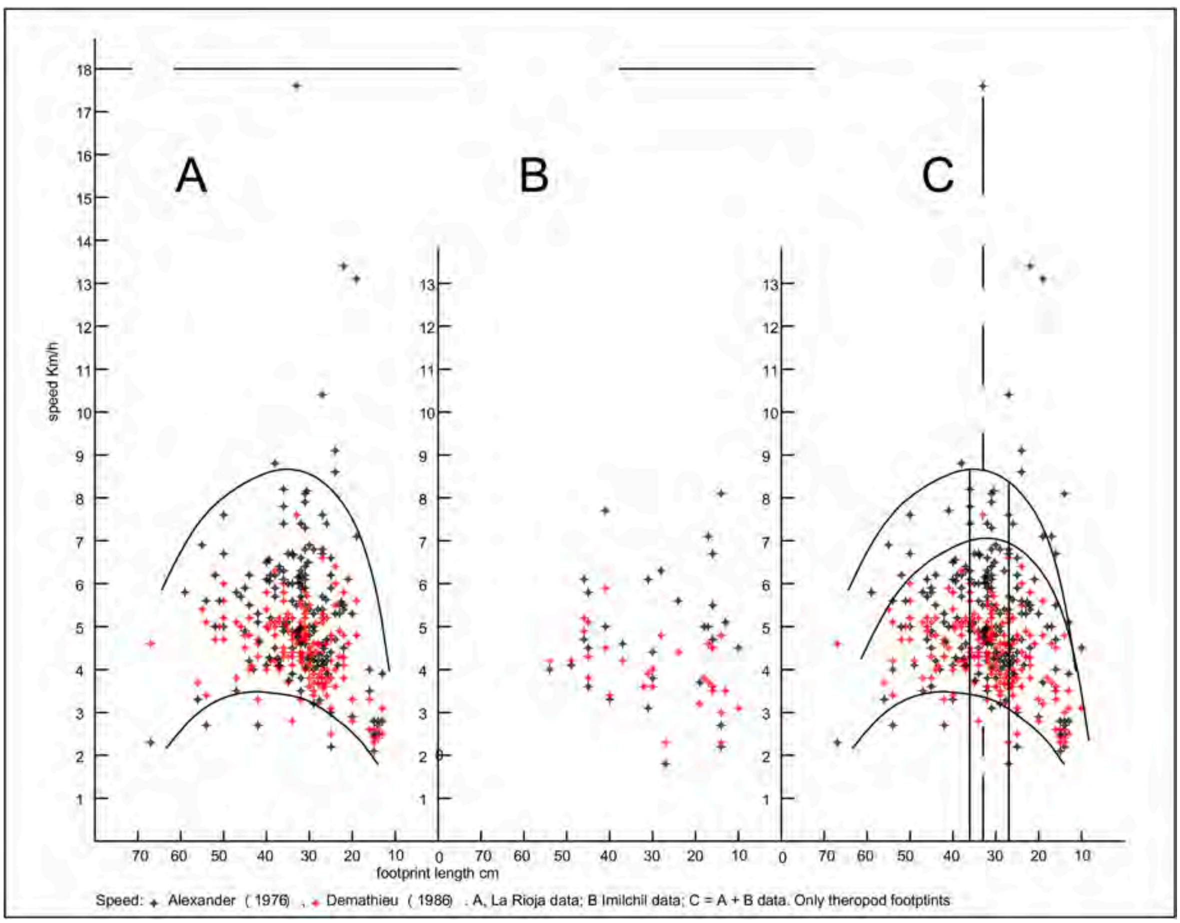

Fig. 25. Projection of the speed as a function of the length of the footprint. The parabolic shape of the cloud indicates that the lower speed is characteristic of the larger footprints and the smaller ones. The average highest speed is located between the large footprints **l** ≈ 30–40 cm.

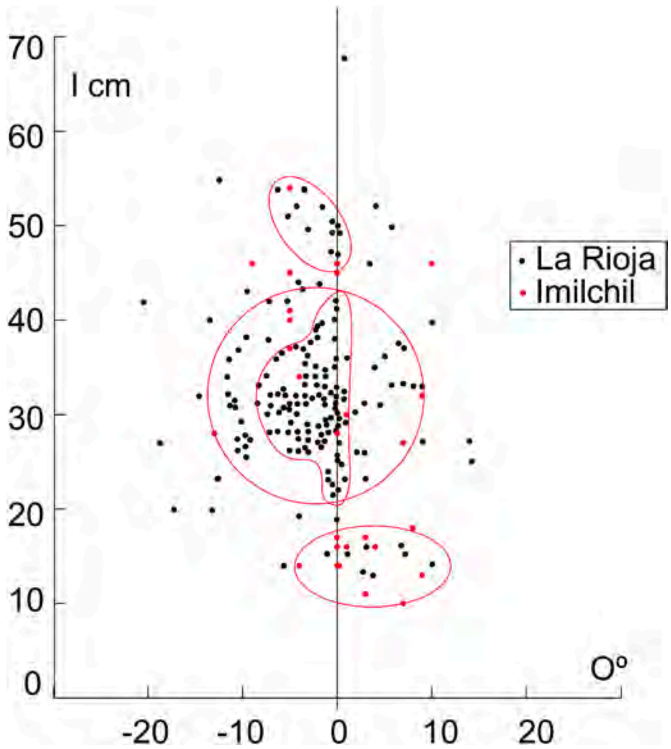

Fig. 26. Projection of the orientation **O** (or axis of the footprints to trackway midline angle) as a function of the footprint length **l**. The same arrangement as in La Rioja is maintained: the smallest footprints tend to positive orientation while the largest ones tend towards negative values.

them. According to several authors (cf. Moratalla and Hernán, 2010), most of the trackway orientation patterns are associated with limits and location of water accumulations.

The sites of the Isli Formation are from fluvial environments (Charrière et al., 2011) so that the observed bidirectionality may depend on the layout of the fluvial courses. Given the paleogeographic conditions of the site, and the fact that the existence of a coastline in the area does not seem possible, it is likely that the directions of travel found in this macrosite are conditioned by the distribution of favorable places in a wet environment. Tail drag traces and crocodile footprints from Imilchil are assumed to be from animals that move in the water (Masrour et al., 2021) and to be of aquatic habits (Masrour et al., 2020) associated with fluvial courses and flooded areas.

The footprints must be found in places with mud, without vegetation that prevents the impression of the autopodia. Additionally, there must be favorable conditions for preservation and fossilization. However, if the accumulation of impressions is maintained in a multitude of strata of a stratigraphic sequence, we must assume that all the conditions have been maintained throughout that sequence.

4.3.3.2. Sigmoid trackways and pace length variation. Two peculiarities that can be observed in the long trackways are the sinuosity of their trajectory and the variation of the pace length ([+] longer and [−] shorter). The first peculiarity was suggested by Leonardi (1979) with the sequence of three footprints to the left and three to the right of an ornithopod trajectory from a trackway in Brazil; the second was shown by Lockley et al. (1994) in a supposedly ornithopod trackway from La Rioja in which long and short paces alternated. Continuing with these observations, Pérez-Lorente (2015) showed several previously described examples in which these peculiarities were examined, in which it is said that:

i) in part, the sigmoid trackways are due to corrections to the variations of the trajectory, to irregularities of the terrain or to the laterality or lameness of the walker (Lockley et al., 1994).
ii) the difference in left and right pace length is normal in trackways, although not always with the same sequence. In the same trackways there are sectors where the long paces are the left ones and other sectors in which the long paces are the right ones.

Until now it has not been determined with certainty if the variation depends exclusively on: anatomical anomalies (Lockley et al., 1994; Razzolini et al., 2016), the curvature of the trajectory, variations in the substrate or correction of the trajectory (cf. Pérez-Lorente, 2015). In Morocco, variations of the trajectory have been shown in theropod trackways (Masrour et al., 2017) and sauropod trackways (Boudchiche et al., 2017).

In Imilchil, trackways with five or more tracks have a sigmoid or irregular trajectory (Fig. 28). The variations in step and stride length, trackway width and step angle are the most sensitive to these variations, which are shown in Table 2. The regular succession of long and short steps is maintained only in 7.1TAG3 and 7.10TAG2. In 5.1TAG5 the trackway begins with increased pace length (the first 5 paces); as is logical, the stride also increases and therefore the speed ($[\mathbf{v_1}+\mathbf{v_2}]/2$ from 4.6 to 5.0 Km/h).

The perfect alternation of long and short steps is easier to find in limited sectors of trackways that are irregular.

5. Conclusions

The tridactyl dinosaur footprints from 14 new Imilchil sites are studied, to which are applied the methods used by us in the analysis of their state of conservation, their ichnotaxonomic determination and in the treatment of metric data and forms.

A large part of the ichnogenera described in Imilchil have been identified by comparing the new footprints found with those described by other authors in this same area. But the morphological variability of the footprints is very large, mainly due to the characteristics of the sediments. The identification has taken into account the morphological variability of the footprints.

Footprints not assignable to ichnogenera are also described. The features of the footprints are shown, both those associated with the anatomical characters of the autopodia and those due to the processes produced during the foot movement and those that modify the original morphology of the action of the foot.

It is also concluded that the metric characters of the footprints and trackways are consistent with those of other sites, highlighting in this sense the existence of a separate group of theropod footprints differentiated by the length of the footprint. We attribute this separation to the presence of dinosaurs that were small in adulthood, and that coexisted in this area with carnivorous dinosaurs of all sizes, even colossal.

Small dinosaur footprints may be of trackmakers that, when adults, do not reach a large size. If we consider the theory of "Ontogenetic Niche Shift" valid, we can suppose that one interpretation of the data leads to the fact that the young of the large dinosaurs were not in this area until they reached a certain size. The analyses of the data from the footprints of Imilchil, are superimposable with those obtained in La Rioja and in Iouaridène, and we assume that the deductions made from them have a universal character.

Declaration of competing interest

The authors declare that they have no known competing financial interests or personal relationships that could have appeared to influence the work reported in this paper.

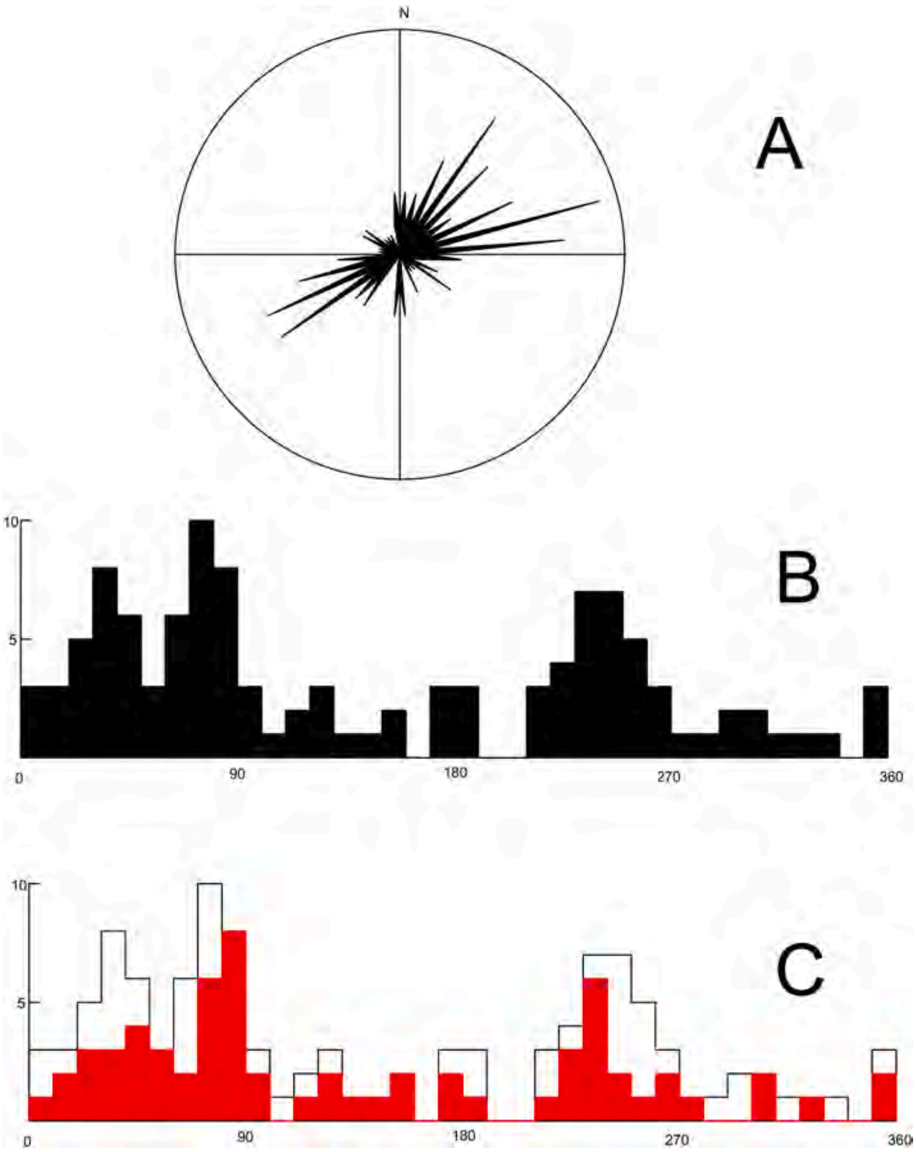

Fig. 27. Projection according to its orientation and direction of isolated footprints, footprint pairs and trackways: A, compass rose (the length of the rays is proportional to the number of data points); B, histogram of number of direction data; C, Histogram without the data of the isolated footprints.

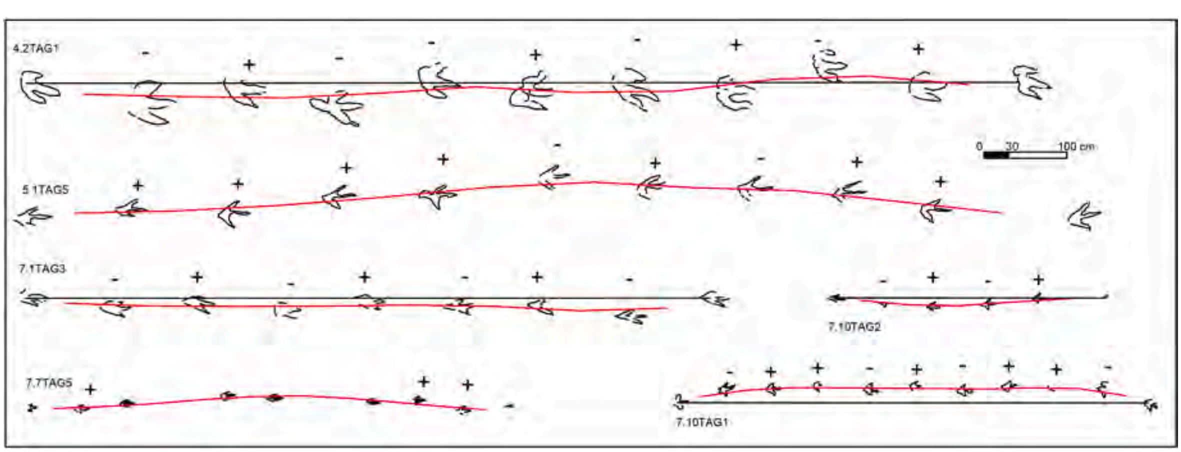

Fig. 28. Irregular and sigmoid trackways of Imilchil. In red, the middle line; in black the line that joins the center of the first and last footprint (pairs and trackways); the signs that indicate the succession of steps short to long (+) and long to short (−). its entire length.

Data availability

No data was used for the research described in the article.

Acknowledgements

We are grateful to the field team formed by Jesús Herrero Gascón from the Guias de Galve association, Ricardo Ochoa Martínez, Carlos Pereda Olásolo and J. Luis Sainz Ruiz de Zuazo, members of the AME association, and Mohamed Alhandaui in the ichnological prospecting and data collection on the Imilchil tracksite. The third author (J. M. C.) was supported by 688 grant PID 2021-124332NB-C22 (Ministerio de Ciencia e Innovación-Agencia Estatal de 689 Investigación, Spain. We thank Raymond Terleckis (BA Spanish) and the anonymous reviewers for their corrections, suggestions and valuable comments.

References

Alexander, N., 1976. Estimates of speed of dinosaurs. Nature 261, 129–130.

Allen, J.R.L., 1997. Subfossil mammañlian tracks (Flandrian) in the Severn Estuary, S.W. Britain: mechanics of formation, preservation and distribution. Phil. Trans. Roy. Soc. Lond. B 352, 481–518.

Boudchiche, L., Masrour, M., Boutakiout, M., Hamzaoui, L., Herrero Gascón, J., Pérez-Lorente, F., 2017. Jarrate Lbel: new Uppper Cretaceous continental site in Morocco. A probable ornitischian non-ornitopod trackway and three amble gait titanosauriform trackways. Geogaceta 6, 9–12.

Boutakiout, M., Hadri, H., Nouri, J., Caro, S., Pérez-Lorente, F., 2006. The syngenetic structure suite of dinosaur footprints in finely laminated sandstones. Site nº 1 of Bin El Oudane (1BO; Central Atlas, Morocco). Ichnos 13, 39–42.

Boutakiout, M., Ladel, L., Díaz-Martínez, I., Pérez-Lorente, F., 2009. Prospecciones paleoicnológicas en el sinclinal de Iouaridème (Alto Atlas, Marruecos). 2: parte oriental. Geogaceta 47, 33–36.

Boutakiout, M., Masrour, M., Pérez-Lorente, F., 2020. New sauropod morphotype definition in the oriental section of Imilchil megatracksite, High Atlas (Morocco). J. Afr. Earth Sci. 161, 1–13. https://doi.org/10.1016/j.jafrearsci.2019.103664.

Brown, T., 1999. The Science and Art of Tracking. Berkley Books, New York, p. 219.

Casamiquela, R.M., 1964. Estudios icnológicos. Problemas y métodos de la icnología con aplicación al estudio de pisadas mesozoicas (Reptilia, Mammalia) de la Patagonia. Publicaciones del Ministerio de Asuntos Sociales, Rio Negro, (-), p. 229.

Casanovas, M.L., Ezquerra, R., Fernández, A., Pérez-Lorente, F., Santafé, J.V., Torcida, F., 1993. - Icnitas de dinosaurios. Yacimientos de Navalsaz, Las Mortajeras, Peñaportillo, Malvaciervo y la Era del Peladillo 2. (La Rioja. España). Zubia - Monogr. 5, 9–133.

Casanovas, M.L., Ezquerra, R., Fernández, A., Montero, D., Pérez-Lorente, F., Santafé, J. V., Torcida, F., 1995. El yacimiento de La Canal (Munilla, La Rioja, España). La variación de velocidad en función del tamaño del pie de los ornitópodos. Zubia 13, 55–81.

Casanovas, M.L., Fernandez, A., Perez-Lorente, F., Santafé, J.V., 1989. - Huellas de dinosaurios de La Rioja.Yacimientos de Valdecevillo, La Senoba y de la Virgen del Campo. I.E.R. Ciencias Tierra 12, 1–190.

Charrière, A., Haddoumi, H., 2016. Les «Couches rouges» continentales jurassico-crétacées des Atlas marocains (Moyen Atlas, Haut Atlas central et oriental): bilan stratigraphique, paléogéographies successives et cadre géodynamique. Bol. Geol. Min. 127, 407–430.

Charrière, A., Ibouh, H., Haddoumi, H., 2011. Le Haut Atlas Central de Beni Mellal à Imilchil. In: Michard, A., Saddiqi, O., Chalouan, A., Rjimati, E., Mouttaqi, A. (Eds.), Le Moyen Atlas. Charrière, A., Ouarhache, D., El-Arabi, H. Nouveaux guides geologiques et miniers du Maroc. *Notes et Mémoires du Service Géologique du Maroc*, vol. 559, p. 162.

Demathieu, G., 1970. Les empreintes de pas de vertebrés du trias de la bordure nord-est du Massif Central. Cah. Palaontol. 11, 219.

Demathieu, G.R., 1986. Nouvelles recherches sur la vitesse des vertébrés auteurs des traces fossiles. Geobios 19, 327–333.

Diaz-Martínez, I., Pérez-Lorente, F., Canudo, J.I., Pereda-Suberbiola, X., 2009. Causas de la variabilidad en icnitas de dinosaurio y su aplicación en icnotaxonomía. Actas IV Jornadas internacionales sobre paleontología de dinosaurios y su entorno 207–220.

Doublet, S., 2004. *Contôles tectonique et climatique de l'enregistrement stratigraphique dans un bassin continental de rift: le bassin de Cameros* Thèse Université de Bourgogne. Memoire, p. 497.

Ellenberger, P., 1970. Les niveaux paléontologiques de première apparition des mammifères primordiaux en Afrique du sud et leur ichnologie. Establissement de zones stratigraphiques detaillées dans le Stormberg du Lesotho (Afrique du Sud) (Trias supérieur à Jurassique). In: Second Gondwana Symposium, Proceedings and Papers. Council for Scientific and Industrial Research, Pretoria, pp. 343–370.

Gandini, J. 2009-2015. http://www.prehistoire-du-maroc.com/taghighacht-imilchil.html.

García-Ramos, J.C., Piñuela, L., Lires, J., 2002. Icnitas de dinosaurios, tipos de sedimentos y consistencia del sustrato. In: Pérez-Lorente, F. (Ed.), Resúmenes del Congreso internacional sobre dinosaurios y otros reptiles mesozoicos en España, pp. 25–26.

Gatesy, S.M., 2003. Direct and indirect tracks features: what sediment did a dinosaur touch? Ichnos 10, 91–98.

Gatesy, S.M., Falkingham, P.L., 2020. Hitchcock's Leptodactyli, penetrative tracks, and dinosaur footprint diversity. J. Vertebr. Paleontol. 40 (3), e1781142 https://doi.org/10.1080/02724634.2020.1781142.

Gierliński, G.D., 2016. Middle Jurassic avialan footprints from lmilchil in Morocco. In: Baucon, A., Neto de Carvalho, C., Rodrigues, J. (Eds.), Ichnia 2016, Abstract Book. UNESCO Geopark Naturtejo/International Ichnological Association Castelo Branco, pp. 98–99.

Gierliński, G.D., Lagnaoui, A., Klein, H., Saber, H., Oukassou, M., Charrière, A., 2017. Bird-like tracks from the Imilchil formation (middle jurassic, bajocian bathonian) of the central high Atlas, Morocco. In: Comparison with Similar Mesozoic Tridactylous Ichnotaxa, vol. 56. Bolletino Società Paleontogica Italiana, pp. 207–215.

Gierliński, G.D., Menducki, P., Janiszewska, K., Wicik, I., Boczarowski, A., 2009. A preliminary report on dinosaur track assemblages from the Middle Jurassic of the Imilchil area, Morocco. Geol. Q. 53 (4), 477–482.

Hadri, M., Pérez-Lorente, F., 2012. Historia de yacimientos con huellas de dinosaurio, desde su descubrimiento hasta su primer estudio. Alrededores de El Mers (Marruecos). Zubia 30, 93–140.

Haubold, H., 1971. Ichnia amphibiorum et reptiliorum fossilium. In: Kuhn, O. (Ed.), Handbuch der Paläoherpetologie, vol. 18, pp. 1–124, 18.

Klein, H., Gierliński, G.D., Oukassou, M., Saber, H., Lallensack, J.N., Lagnaoui, A., Hminna, A., Charrière, A., 2022. Theropod and ornithischian dinosaur track assemblages from middle to ?late jurassic deposits of the central high Atlas, Morocco. Hist. Biol. https://doi.org/10.1080/08912963.2022.2042808.

Klein, H., Lagnaoui, A., Gierliński, G.D., Saber, H., Oukassou, M., Charrière, A., 2017. Crocodylomorph and turtle footprints in dinosaur-dominated Middle Jurassic and ? Lower-mid-Cretaceous ichnoassemblages of the Central High Atlas and High Moulouya regions, Morocco – ichnotaxonomy, trackmakers and implications for paleoecology. In: 2nd *International conference on continental ichnology. Nuy Valley. Africa del Sur. Abstract book*, pp. 45–s.

Klein, H., Lagnaoui, A., Gierliński, G.D., Saber, H., Lallensack, J.N., Oukassou, M., Charrière, A., 2018a. Crocodylomorph, turtle and mammal footprints in dinosaur-dominated Middle? Upper Jurassic and mid-Cretaceous ichnoassemblages of Morocco. Palaeogeogr. Palaeoclimatol. Palaeoecol. 498, 39–52.

Klein, H., Lagnaoui, A., Gierliński, G.D., Saber, H., Oukassou, M., Charriere, A., 2018b. Crocodylomorph and turtle footprints in dinosaur-dominated Middle Jurassic and ? Lower-mid-Cretaceous ichnoassemblages of the Central High Atlas and High Moulouya regions, Morocco – ichnotaxonomy, trackmakers and implications for palaeoecology. In: Proceedings of the 2nd International Conference of Continental Ichnology (ICCI 2017), vol. 52. Paleontología africana, pp. 169–170.

Leonardi, G., 1979. Nota preliminar sobre seis pistas de dinosaurios Ornithischia da Bacia do Rio de Peixe em Sousa, Paríba, Brasil. An. Acad. Bras. Cienc. 51, 501–516.

Leonardi, G. (Ed.), 1987. *Glossary and Manual of Tetrapod Footprint Palaeoichnology*. Republica Federativa do Brasil Ministerio das Minas e Energia. Departamento Nacional da Producão Mineral, Brasilia, p. 75.

Lessertisseur, J., 1955. Traces fossiles d'activité animale et leur signification paléobiologique, vol. 74. Mémoire Société Géologique de France, pp. l–150 nouv sér.

Lockley, M.G., Hunt, A.P., Moratalla, J.J., Matsukawa, M., 1994. - Limping Dinosaurs? Trackway Evidence for Abnormal Gaits. Ichnos, pp. 193–202.

Lockley, M.G., Meyer, C.A., Santos, V.F., 1998. *Megalosauripus* and the problematic concept of *Megalosaur* footprints. Gaia 15, 313–317.

Lockley, M.G., 1991. Tracking Dinosaurs: a New Look at an Ancient World. Cambridge Univ. Press, p. 238.

Lockley, M.G., Xing, L., 2015. Flattened fossil footprints: implications for paleobiology. Palaeogeogr. Palaeoclimatol. Palaeoecol. 426, 85–94. https://doi.org/10.1016/j.palaeo.2015.03.008.

Lockley, M.G., Xing, L., 2021. A review of the non-avian theropod track record and the implications for the Ontogenetic Niche Shift model. Earth Sci. Rev. 220 https://doi.org/10.1016/j.earscirev.2021.103715.

Lockley, M.G., Young, B.H., Carpenter, K., 1983. Hadrosaur locomotion and herding behavior: evidence for footprints of the Mesaverde Formation, Grand Mesa coal field, Colorado. Mt. Geol. 20, 5–14.

Martin Escorza, C., 1988. Orientación de las icnitas en el valle del Cidacos (La Rioja). Bol. R. Soc. Esp. Hist. Nat. Actas 84, 32–34.

Martin Escorza, C., 2001. Orientación de las icnitas de dinosaurios en la Sierra de Cameros. Zubia 19, 139–163.

Marty, D., Belvedere, M., Razzolini, N.L., Lockley, M.G., Paratte, G., Cattini, M., Lovis, C., Meyer, C.A., 2017. The tracks of giant theropods (Jurabrontes curtedulensis ichnogen. & ichnosp. nov.) from the Late Jurassic of NW Switzerland: palaeoecological & palaeogeographical implications. Hist. Biol. https://doi.org/10.1080/08912963.2017.1324438.

Masrour, M., Boutakiout, M., Herrero Gascón, J., Ochoa Martínez, R., Sáinz Ruiz de Zuazu, J.L., Pérez-Lorente, F., 2021. Crocodile tail traces and dinosaur footprints. Bathonian?-Callovian. Imilchil. High Central Atlas. Morocco. Geogaceta 69, 95–98.

Masrour, M., Boutakiout, M., Herrero Gascón, J., Sáinz Ruiz de Zuazo, J.L., Ochoa Martínez, R., Pérez-Lorente, F., 2020. Footprints of *batrachopus isp.* from the Imilchil megatracksite, upper jurassic, central high Atlas (Morocco). J. Afr. Earth Sci. 172.

Milan, J., Bromley, R.G., 2006. True tracks, undertracks and eroded tracks, experimental work with tetrapod tracks in laboratory and field. Palaeogeogr. Palaeoclimatol. Palaeoecol. 231, 253–264.

Minguez Ceniceros, J., Farlow, J.O., Masrour, M., Extremiana, J.I., Boutakiout, M., Pérez-Lorente, F., 2022. Demographic interpretarion of colosal theropod footprints discoveries from Imilchil (Mid-Jurassic, central high Atlas, Morocco). J. Afr. Earth Sci. 193 https://doi.org/10.1016/j.jafrearsci.2022.104595.

Moratalla, J.J., Hernán, J., 2010. Probable palaeogeographical influences of the Lower Cretaceous Iberian rifting phase in the eastern Cameros Basin (Spain) on dinosaur trackway orientations. Palaeogeogr. Palaeoclimatol. Palaeoecol. 295, 116–130.

Masrour, M., Lkebir, N., Pérez-Lorente, F., 2017. Anza palaeoichnological site, Late Cretaceous, Morocco. Part II. Problems of large dinosaur trackways and the first African Macropodosaurus trckway. J. Afr. Earth Sci. https://doi.org/10.1016/j.jafrearsci.2017.04.019.

Oukassou, M., Klein, H., Lagnaoui, A., Charrière, A., Saber, H., Gierliński, G.D., Lallensack, J.N., Hminna, A., Boumaalif, A., Oussou, A., Ouarhache, D., 2019a. *Polyonyx*-like tracks from Middle-?Upper Jurassic red beds of Morocco: implications for sauropod communities on southern margins of Tethys. Palaeogeogr. Palaeoclimatol. Palaeoecol. https://doi.org/10.1016/j.palaeo.2019.109394.

Oukassou, M., Lagnaoui, A., Charrière, A., Saber, H., Bel Haouz, W., Gierliński, G.D., Klein, H., Ibouh, H., 2019b. New evidence of xiphosurids from the Middle Jurassic of Morocco: palaeoenvironmental, palaeoecological and palaeobiogeographical implications. Palaeogeogr. Palaeoclimatol. Palaeoecol. 516, 268–283. https://doi.org/10.1016/j.palaeo.2018.11.034.

Peabody, F.E., 1955. Taxonomy and the footprints of tetrapods. J. Paleontol. 29, 915–918.

Pérez-Lorente, F., 1996. Pistas terópodas en cifras. Zubia 14, 37–55.

Pérez-Lorente, F., 2001. Paleoicnología. Los dinosaurios y sus huellas en La Rioja. Apuntes para los cursos y campos de verano. Gobierno de La Rioja, p. 227.

Pérez-Lorente, F., 2003. Aportaciones de los yacimientos de Las Barguillas, Santisol y Santa Julians (Hornillos de Cameros, La Rioja, España). In: Pérez-Lorente (Ed.), Dinosaurios y otros reptiles mesozóicos en España, vol. 26. Ciencias de la Tierra, pp. 161–194.

Pérez-Lorente, F., 2015. Dinosaur footprints and trackways of La Rioja. In: Farlow, J.O. (Ed.), Life of the Past. Indiana University Press, p. 363.

Pérez-Lorente, F., Romero-Molina, M.M., 2001. Icnitas terópodas del Cretácico Inferior de La Rioja (España). Zubia 19, 115–118.

Pérez-Lorente, F., Romero-Molina, M.M., Pereda Olásolo, J.C., 2000. Icnitas ornitópodas del Contadero (Torremuña, La Rioja, España). Estructuras de barro y baja velocidad de marcha. Tomo homenaje a J. L. Fernández Sevilla y M. Balmaseda Aróspide.. IER. 17–28.

Razzolini, N., Vila, B., Diaz-Martínez, I., Manning, P.L., Galobart, A., 2016. Pes shape variation in an ornithopod dinosaur trackway (Lowe Cretaceous, NW Spain): new evidence of an antalgic gait in the fossil track record. Cretac. Res. 58, 125–134.

Requeta, L.E., Hernández Medrano, N., Pérez-lorente, F., 2006-2007. - La Pellejera: descripción y aportaciones. Heterocronía y variabilidad de un yacimientos con huellas de dinosaurio de La Rioja (España). Zubia - Monogr. (18–19), 21–114.

Romero-Molina, M.M., Pérez-Lorente, F., Rivas, P., 2003. Análisis de la parataxonomía utilizada con las huellas de dinosaurio. In: Dinosaurios y otros reptiles mesozoicos de España. Pérez-Lorente, vol. 26. F. coord. Ciencias de la Tierra, pp. 13–32.

Sarjeant, W.A.S., 1989. Ten ichnological commandments: a standardized procedure for the description of fossil vertebrate footprints. In: Gillette, D.D., Lockley, M.G. (Eds.), *Dinosaur Tracks and Traces*: Cambridge. Cambridge University Press, pp. 369–370.

Sarjeant, W.A.S., 1990. - A name for the trace of an act: approaches to the nomenclature and classification of fossils vertebrate footprints. In: Carpenter y, K., Currie, P.J. (Eds.), Dinosaur Systematics: Perspectives and Approaches. Cambridge Univ. Press, pp. 299–308.

Schroeder, K., Lyons, S.K., Smith, F.A., 2021. The influence of juvenile dinosaurs on community structure and diversity. Science 371, 941–944.

Shell, R., Boss, S.K., 2013. Morphometric analysis of dinosaur tracks from Southwest Arkansas. J. Arkansas Academy Sci. 67, 1–24.

Sternberg, C.M., 1926. Dinosaur tracks from the edmonton formation of alberta. Canada department of mines. geological series 46 Geol. Surv. Bull. 44, 85–87, 134-135.

Thulborn, R.A., 1990. - *Dinosaur Tracks*. Chapman and Hall, p. 410.

Thulborn, R.A., Wade, M., 1989. A footprint as a history of movement. In: Gillette y, D. D., Lockley, M.G. (Eds.), En *Dinosaurs Tracks and Traces*. Cambridge Universikty Press, pp. 51–56.

Young, C.C., 1960. Fossil footprints in China. Vertebr. Palasiat. 4, 53–66.